10

Biomimetics - Thermodynamics to Study Wetting of Self-Cleaning Surfaces

Erwin Hüger, Jürgen Rost, Marion Frant, Gerhard Hildebrand, and Klaus Liefeith
Department of Biomaterials, Institute for Bioprocessing and Analytical Measurement Techniques (iba) e.V., Rosenhof, D-37308 Heilbad Heiligenstadt Germany

1. Introduction

Brilliant, recyclable and always surprising are the inventions of nature. Hence, it is no wonder that industry attempts to imitate natural environments. However, there is not a single engine that can keep up with the low-consumption of a hummingbird, and there are no paints available that are as permanently clean as a lotus leaf. The lotus effect relies on a strong water repellency. Rain drops have an almost spherical shape on the lotus leaf with minuscule contact area of low adhesion. Hence, the drops easy roll-up collecting dust and pathogens, cleaning in that way the leaf surface. One of the most important reasons for the existence of water-repellent natural surfaces is that it provides protection against pathogens supplied by free water such as bacteria or fungal spores. Therefore, water removal minimizes the chances of infection. In addition, dust particle removal from natural surfaces minimizes organism overheating or salt injury. However, surfaces of self-cleaning plants and insects are not the only example from nature for water repellency. Due to humidity, all surfaces are less or more covered by a nanoscopic thick water layer. In general, water environments are a frequent habitate on our blue planet. Hence, water repellency is long-established in nature. Feather of e.g. terrestrial birds have evolved primarily to repeal water (Rijke & Jesser, 2010).

Although nature still offers the best self-cleaning-properties by its remarkable ability for self-healing, there is a huge effort to constructing artificial biomimetic superhydrophobicity. Extreme water-repellency as well as extreme water-wetting properties are of considerable technological interest with a high-potential for energy economization. For example, extreme water-repellency is the basis for self-cleaning and anti-fouling which are the objects of a fast-growing research field with a multitude of applications in goods used every day. On the other hand, liquid-wetting and the dewetting-resistance are useful for tissue-engineering and implants where the biological cells need an aqueous environment. Accordingly, currently there is an intensified endeavor in research and development of materials with strong wetting and dewetting resistance. A huge number of studies have been carried out to produce artificial biomimetic roughness-induced superhydrophobic surfaces. A valuable recent review published by InTech (Qu & He & Zhang, 2010) is worth mentioning here.

We show that a simply constructed Gibbs-energy expression for the system composed of a liquid-droplet on material surfaces can adequately determine the water-repellency or water-absorbency in dependence of the surface structure and chemistry. The calculations do

not need exceptional computational facilities and, in fact, do not even require computational knowledge. Since biomimetics has evolved into an interdisciplinary field of research, this chapter addresses scientists involved in engineering, chemistry, physics, biology, botany and related subjects, engaged in both academia or industry.

Up-to date wettability calculations are restricted to theoretically-modeled surface morphology, where the morphology is considered to be an identically repetition of one and the same asperity feature, e.g. pillars, (homogeneously dispersed) on the surface (Barbieri & Wagner & Hoffmann, 2007; Patankar, 2004; 2003; Nosonovsky & Bhushan, 2005; 2006; Ishino & Okumura, 2006). Real surfaces do not possess only one kind of asperity geometry, but a diversity of roughness features often randomly dispersed on the material surface. We apply our equations on real surfaces. For that reason we select the surface of *Colocasia esculenta* plant leaves which are evolution-optimized for self-cleaning property through natural selection. We determine experimentally the surface morphology of the *Colocasia esculenta* leaf surface with atomic force microscopy of a special setup designed for experiments in LifeScience (Huger, 2009). Using Gibbs-energy calculations we determine metastable and equilibrium states during the wetting of *Colocasia esculenta* leaf surface. However, the experiments are terestial. To make the calculations even more realistic, the gravitational force will be included in the Gibbs energy function. Liquid drops sitting or hanging from textured surfaces will be considered as well as the type of liquids. Illustrative graphical presentations as well as analytical minimization of the Gibbs-energy function as a function of the surface roughness, surface chemistry and acting forces will be provided.

This chapter focusses on the description of the Gibbs energy formula for wetting analysis with application on the evolution-optimized self-cleaning *Colocasia esculenta* leaf surface. To that purposes the chapter is organized as follows: Section (2) gives a brief description to the interaction of the liquid drop molecules to vapor (e.g. air) and material surfaces. In section (3) the Gibbs energy of a liquid drop on a material surface is constructed. Special emphasis will be given to the constituents of the Gibbs energy function that can be determined experimentally and how unavowed components can be expressed by experimentally procurable values, or avoided in order to solve the equations. Approaches will be discussed. After that, the Gibbs energy function will be built up step by step by considering flat (section (4)), rough (section (5)) and composite (section (6)) surfaces. Special attention will be given to the effect of gravitational fields. It will be shown how the surface morphology and surface chemistry enters the equations. Gibbs energy maps and Gibbs energy minimizations will illustratively explain the Wenzel (wetting) regime and the Cassie-Baxter (partial-wetting) equation. Section (6) will show how the constructed Gibbs energy function can be applied on a real system composed by the self-cleaning *Colocasia esculenta* leaf. Illustrative images will explain how the roughness parameters are extracted from the experimental data to enter the Gibbs energy function. The gravitational contribution will be included for drops resting on or hanging from the plant leaves. Our conclusion and outlook will be summarized in section (7). Limitations of the current model will be expressed.

2. Hydrophilic and hydrophobic interraction. Contact-angle.

Interaction of substances to water molecules (i.e. hydrophilicity and hydrophobicity) plays a crucial role in biological cell building and functionality, hydrophobic and hydrophilic interaction being the succesful strategy of life-fountain. Furthermore, the bond strength to water molecules plays also a role for evolution-optimized macroscopic properties of life-form such as the mentioned self-cleaning plant leafs and feather evolution.

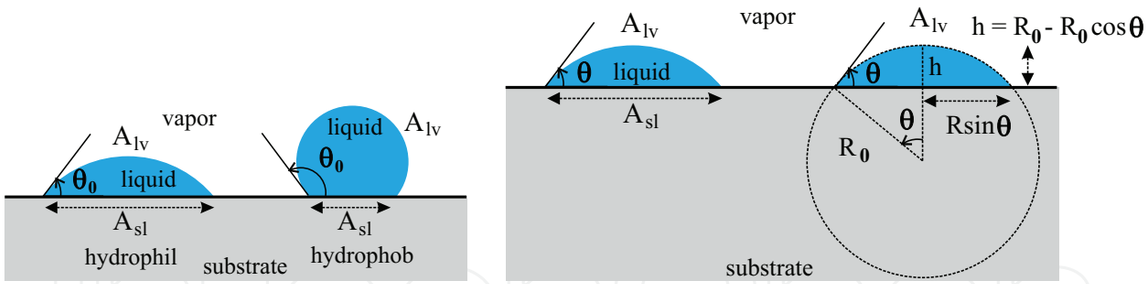

Fig. 1. Left sketch: Contact angle of a liquid drop on a substrate. Right panel: The liquid droplet is a spherical dome.

Water repellency can be conveniently expressed by the contact angle θ, defined as the angle between the tangent to the curved water surface at the point of contact with the solid surface and the plane of the surface on which the drop is resting, measured through the water (Fig. 1) (Marmur, 2010).
Hydrophilic materials "like" the contact with water due to a gain in energy at the material-water interface. In contrast, a water repellent surface (hydrophobic surface) "hates" the contact with water due to an increase in energy at the water-material interface, or a lower decrease in energy for drops in contact to hydrophobic chemistry in comparison to drops in contact with hydrophilic materials. Consequently, a water-repellent surface seeks to minimize the contact with water as far as possible, whereby a hydrophilic surface seeks to maximize its contact area with water. Hydrophilic surfaces are very common in industrial application and environment. For example, all metals and almost all oxides are intrinsically hydrophilic from nature. In contrast, hydrophobic surfaces are much more rare to be found. A hydrophobic surface is a surface with very low surface free energy. Low-energy surfaces can be obtained by saturated fluor (Hunter, 2010) and sulphur (Huger, 2008) bonds, both of them being poissoners.
The contact angle of water droplet which forms on a hydrophobic (hydrophilic) surface (see Fig. 1) is a result of energy minimization of the system built up by the surface material, liquid (e.g. water) droplet and gas environment (e.g. air) and is successfully related by the Youngs equation:

$$\cos\theta_0 = \frac{\sigma_{sv} - \sigma_{sl}}{\sigma_{lv}} \tag{1}$$

where θ_0 is the intrinsic contact angle, called also the Young contact angle, σ is the surface tension and the subscripts s, l and v denote the solid, liquid (e.g. water) and vapor (e.g. air) phase. Hydrophilic (hydrophobic) surfaces force the liquid droplet to have contact angles with more (less) than 90 degrees. Up to date there is no chemistry which allows a smooth surface to be built up at a water contact-angle larger than 120 degrees (Hunter, 2010). However, the contact angle measured on so-called superhydrophobic surfaces is larger than 150 degrees. The surface morphology and not the chemistry have to be the reason for such high contact-angles.
Super-repellent surfaces are that class of superhydrophobic surfaces on which water-droplets are not sticky. Hence, on such surfaces the droplets can easily roll-off already at a small inclination of no more than a few degrees. Such surfaces possess then self-cleaning properties, i. e. the possibility to roll-off of a water droplet under even a tiny disturbance taking the dust adhered to it cleaning in that way the surface. The cleaning procedure happens because

usually the dust adheres more strongly on the water drop than on the surface due to the surface liquid tension.
In this chapter we build up the Gibbs free energy of the system under discussion and we will show through the work how valuable results can be obtained by energy minimization on the ground of peculiar surface morphology.

3. Gibbs free energy. Model

3.1 Approach

Thermodynamics is a subject of immense practical value. One reason why thermodynamics is so valuable for physicists, chemists and engineers is that it is a theory which can be developed in its entirity, without gaps in the argument, on the basis of only moderate knowledge of mathematics (Denbigh, 1968). In this spirit, the Gibbs free energy of the system built up by a liquid droplet on a solid surface is given by the sum of the interfacial energies (Huger, 2009):

$$G = A_{lv}\sigma_{lv} + A_{sl}\sigma_{sl} + A_{sv}\sigma_{sv} \tag{2}$$

where A denotes the areas of the liquid-vapor (A_{lv}), solid-liquid (A_{sl}) and solid-vapor interfaces (A_{sv}).
Equation (2) represents a balance between each interfacial energy. Interfaces where the liquid molecules possess low bonding (i.e. hydrophobic interaction) increases the total interfacial energy. Hydrophilic interaction reduces the energy. So, the liquid drop would try to minimize its interface to air (vapor) (A_{lv}) and to maximize the solid-liquid interface (A_{sl}). The increase of the solid-liquid interface would reduce the energy, but would also change the drop shape. The drop-shape change can increase the interface to air (vapor) (A_{lv}) and, consequently, increase the energy. The system can reach such a wetting state, where the energy reduction by a growth of the solid-liquid interface is lower than the energy increase by the accompanied drop-shape change. There, the drop-shape lies in metastable or global energy minima. So, total energy minima appears for specific drop shapes and wetting behaviour. This is the aim of thermodynamics, which focuses on the description of equilibrium properties. Energy calculations are performed to analytically or numerically predictable local or global equilibrium properties (Cool & Garcia, 2010; Huger & Sob, 2010). In that spirit, we intend to find out how drop shapes and wetting behaviours influences the total interfacial energy.
Now, the interface areas can be determined. σ_{lv} can be measured, but σ_{sl} and σ_{sv} are unknown (Chaudhury & Whitesides, 1992). However, from equation 1 one can get the difference:

$$\sigma_{sv} - \sigma_{sl} = \sigma_{lv}\cos\theta_0 \tag{3}$$

So, in order to be able to calculate the Gibbs energy of the system under study it is necessary to express the Gibbs energy function to be dependent only on the difference between σ_{sl} and σ_{sv}. Fortunately, this can be done easily.
A_{sv} is the difference between the total area A_{tot} of the material surface and the area of the wetted material surface A_{sl}:

$$A_{sv} = A_{tot} - A_{sl} \tag{4}$$

From equations (2) and (4) one obtains:

$$G - A_{tot}\sigma_{sv} = A_{lv}\sigma_{lv} + A_{sl}(\sigma_{sl} - \sigma_{sv}) \tag{5}$$

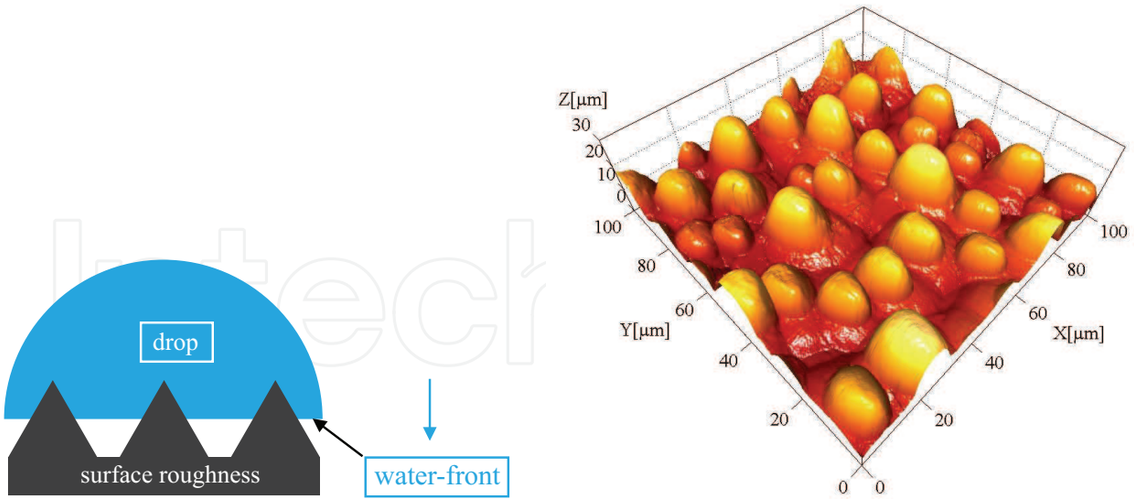

Fig. 2. Left panel: Schematic representation of a Cross-section through a liquid-droplet penetrating surface asperities. Right image: Atomic force microscopy from Colocasia esculenta leaf.

and using the equation (3) follows:

$$E = G - A_{tot}\sigma_{sv} = A_{lv}\sigma_{lv} - A_{sl}\sigma_{lv}\cos\theta_0 \tag{6}$$

Now, the term $A_{tot}\sigma_{sv}$ is constant during the behavior of the liquid droplet on the material surface, whereas the other terms of equation (6) depends on the droplet state on the surface. Fortunately, all terms on the right part of the equation (6) can be determined. It makes no difference if the Gibbs energy G or the difference $E = G - A_{tot}\sigma_{sv}$ is used for calculations, since metastable and equilibrium drop shape are obtained by energy minimization:

$$0 = \frac{\partial E}{\partial \theta} = \frac{\partial (G - A_{tot}\sigma_{sv})}{\partial \theta} = \frac{\partial G}{\partial \theta} = \frac{\partial (A_{lv}\sigma_{lv} - A_{sl}\sigma_{lv}\cos\theta_0)}{\partial \theta} \tag{7}$$

So, in the following we will calculate the energy difference E expressed in eq. (6). Before doing so, we will take gravity into account.

3.2 Gravity contribution

The experiments on drops done so far are terrestrial. For very small drops the gravity field can be neglected due to the larger contributions from surface tension, but, as it will be further shown, for larger drops the gravity contribution becomes relevant. The gravity contribution to the total Gibbs energy will be investigated for drops resting on surfaces or hanging from surfaces. In the following we will take into account drops whose size is much larger than the size of the surface roughness feature. The water front penetrating the surface roughness is taken as a horizontal plane, as depicted in the left sketch of Fig. 2. The right panel of Fig. 2 presents an atomic force microscopy (AFM) image of the *Colocasia esculenta* leaf surface.
The surface contains surface protrusions called papillae. The distance between the highest papillae extends up to 40 μm. So, the radius of the droplet base (see Fig. 1) should be equal at least to $R\sin\theta = 80\mu m$. In our laboratory we measured a contact angle of $\theta = 170^o$ for the leaf surface presented in Fig. 2. Hence, the radius of the liquid droplet should be some 460 μm. Consequently, the volume of the droplet considered through this work should be at least some

0.4 μl. However, in our laboratory we routinely used liquid droplets of 3 to 5 μl for contact angle measurments, the drop bases of which contacts a lot of leaf papillae.
For large droplets, the center of mass will strongly depend on the drop contact angle. A lower contact angle (θ) means that the center of mass will be lower and the systems lowers in that way its total energy. So, the θ-dependent part of the gravity is given by:

$$E_g(\theta) = mgC_z(\theta) = \rho V g C_z(\theta) \tag{8}$$

where m is the mass of the drop, V the drop volume, ρ the liquid density, g the gravity acceleration and C_z the vertical position of the drop mass-center.
In the case the drop is homogeneously filled by the liquid, the drop mass-center is given by the formula for the centroid of solids:

$$C_z = \frac{1}{V}\int_V z dV = \frac{1}{V}\int_{zmin}^{zmax} z\frac{\partial V(z)}{\partial z}dz \tag{9}$$

The drop is a spherical dome where $zmax = h$ (see Fig. 1). $zmin = 0$ can be selected. $V(z)$ is the volume of the drop from $zmin = 0$ up to the vertical value z. For $zmax = h$ the volume is given by:

$$V(zmax) = \pi R_0 h^2 - \frac{1}{3}\pi h^3 = \frac{\pi R_0^3}{3}(1-\cos\theta)^2(2+\cos\theta) \tag{10}$$

For an arbitrary value z ($0 < z \leq h$) the volume is given by:

$$V(z) = V(zmax) - V^{dome}(z) = (\pi R_0 h^2 - \frac{1}{3}\pi h^3) - [\pi R_0 (h-z)^2 - \frac{1}{3}\pi (h-z)^3] \tag{11}$$

With $h = R_0(1-\cos\theta)$ (see Fig. 1) follows:

$$\begin{aligned} V(z) &= \frac{\pi R_0^3}{3}(1-\cos\theta)^2(2+\cos\theta) - \frac{\pi}{3}(h-z)^2(3R_0 - h + z) = \\ &= \frac{\pi R_0^3}{3}(1-\cos\theta)^2(2+\cos\theta) - \frac{\pi R_0^3}{3}(1-\cos\theta-\frac{z}{R_0})^2(2+\cos\theta+\frac{z}{R_0}) \end{aligned} \tag{12}$$

With $p = z/R_0$ eq. (12) can be written as:

$$\begin{aligned} V(p) &= \frac{\pi R_0^3}{3}(1-\cos\theta)^2(2+\cos\theta) - \frac{\pi R_0^3}{3}(1-\cos\theta-p)^2(2+\cos\theta+p) \\ &= \frac{\pi R_0^3}{3}(3p\sin^2\theta - 3p^2\cos\theta - p^3) \end{aligned} \tag{13}$$

and consequently:

$$dV = \frac{\partial V}{\partial p}dp = \frac{\pi R_0^3}{3}(3\sin^2\theta - 6p\cos\theta - 3p^2)dp = \pi R_0^3(\sin^2\theta - 2p\cos\theta - p^2)dp \tag{14}$$

From $z = p \cdot R_0$ follows $pmax = h/R_0 = 1 - \cos\theta$ and $pmin = 0$. So, eq. (9) becomes:

$$\begin{aligned} C_z &= \frac{1}{V}\int_V z dV = \frac{1}{V}\int_{pmin}^{pmax} p \cdot R_0 \frac{\partial V(p)}{\partial p} dp = \\ &= \frac{1}{\frac{\pi R_0^3}{3}(1-\cos\theta)^2(2+\cos\theta)} \cdot \int_0^{1-\cos\theta} p \cdot R_0 \cdot \pi R_0^3 (\sin^2\theta - 2p\cos\theta - p^2) dp \\ &= \frac{3R_0[\frac{(1-\cos\theta)^2\sin\theta}{2} - \frac{2}{3}\cos\theta(1-\cos\theta)^3 - \frac{1}{4}(1-\cos\theta)^4]}{(1-\cos\theta)^2(2+\cos\theta)} \\ &= \frac{\frac{3R_0}{12}(5\sin^2\theta + 5\cos^2\theta - 3 + \sin^2\theta - 2\cos\theta)}{(2+\cos\theta)} = \frac{R_0}{4}\frac{(1-\cos\theta)(3+\cos\theta)}{2+\cos\theta} \end{aligned} \tag{15}$$

From eq. (8) and eq. (15) follows the gravity contribution to the total Gibbs energy to be:

$$E_g(\theta) = \frac{\rho V g R_0}{4} \cdot \frac{(1-\cos\theta)(3+\cos\theta)}{2+\cos\theta} \tag{16}$$

With:

$$V = \frac{\pi R_0^3}{3}(1-\cos\theta)^2(2+\cos\theta) \Leftrightarrow R_0 = \left(\frac{3V}{\pi(1-\cos\theta)^2(2+\cos\theta)}\right)^{\frac{1}{3}} \tag{17}$$

follows finally:

$$\begin{aligned} E_g(\theta) = & \quad \frac{\rho V g}{4}\left(\frac{3V}{\pi(1-\cos\theta)^2(2+\cos\theta)}\right)^{\frac{1}{3}} \cdot \frac{(1-\cos\theta)(3+\cos\theta)}{2+\cos\theta} = \\ = & \quad \frac{(3^{\frac{1}{3}})\rho(V^{\frac{4}{3}})g}{4\pi^{\frac{1}{3}}} \cdot \frac{(1-\cos\theta)^{\frac{1}{3}}(3+\cos\theta)}{(2+\cos\theta)^{\frac{4}{3}}} \end{aligned} \tag{18}$$

Now, ρ, V, g are constant. Hence, the gravity contribution (eq. (18)) is dependent only on the drop contact angle (θ).
Finally, the Gibbs energy including the gravity contribution is given by:

$$\begin{aligned} E &= G - A_{tot}\sigma_{sv} = A_{lv}\sigma_{lv} - A_{sl}\sigma_{lv}\cos\theta_0 + E_g(\theta) = \\ &= A_{lv}\sigma_{lv} - A_{sl}\sigma_{lv}\cos\theta_0 + \frac{(3^{\frac{1}{3}})\rho(V^{\frac{4}{3}})g}{4\pi^{\frac{1}{3}}} \cdot \frac{(1-\cos\theta)^{\frac{1}{3}}(3+\cos\theta)}{(2+\cos\theta)^{\frac{4}{3}}} \end{aligned} \tag{19}$$

The following sections apply the Gibbs formula without (eq. (6)) and include the gravity (eq. (19)) on flat and rough surfaces.

4. Flat surfaces

4.1 Without gravity contribution

In the case of a flat surfaces, the liquid-vapor interface is considered to be a spherical cap, the curvature surface of a spherical dome (see Fig.1). The surface area of a spherical dome's ceiling is:

$$A_{lv} = 2\pi R_0 h = \pi R_0^2 (2 - 2\cos\theta) \tag{20}$$

where R_0 is the radius of curvature and θ is an arbitrary contact angle imposed to the drop and not necessarily its equilibrium contact angle (should be used in the minimization of Gibbs energy).
The area of the solid-liquid interface is equal to the area of the spherical dome base:

$$A_{sl} = \pi (R_0 \sin\theta)^2 \tag{21}$$

Introducing relation (20) and (21) into the equation (6) of the Gibbs energy follows:

$$\frac{G - A_{tot}\sigma_{sv}}{\pi R_0^2 \sigma_{lv}} = 2 - 2\cos\theta - (\cos\theta_0)\sin^2\theta \tag{22}$$

Now, a change in θ changes also R_0. In order to work with a constant value, R_0 will be expressed by the volume V of the drop which is constant during the drop shape change. From the volume of the drop (spherical dome) eq. (10) follows:

$$\frac{G - A_{tot}\sigma_{sv}}{\pi (\frac{3V}{\pi})^{\frac{2}{3}} [(1-\cos\theta)^2(2+\cos\theta)]^{-\frac{2}{3}} \sigma_{lv}} = 2 - 2\cos\theta - (\cos\theta_0)\sin^2\theta \tag{23}$$

and finally:

$$\frac{G - A_{tot}\sigma_{sv}}{\pi \sigma_{lv} (\frac{3V}{\pi})^{\frac{2}{3}}} = [(1-\cos\theta)^2(2+\cos\theta)]^{-\frac{2}{3}} \cdot (2 - 2\cos\theta - \cos\theta_0 \sin^2\theta) \tag{24}$$

In the left side of equation (24) all values up to G are constant during the behavior of a droplet on the surface. Consequently we can put:

$$G - A_{tot}\sigma_{sv} = E \tag{25}$$

and hence calculate the energy E:

$$E(\theta,\theta_0) = (\pi \sigma_{lv} (\frac{3V}{\pi})^{\frac{2}{3}}) [(1-\cos\theta)^2(2+\cos\theta)]^{-\frac{2}{3}} \cdot (2 - 2\cos\theta - \cos\theta_0 \sin^2\theta) \tag{26}$$

With

$$\Phi(\theta_0) = \Phi_{smooth}(\theta_0) = \cos\theta_0 \tag{27}$$

and

$$F(\theta) = [(1-\cos\theta)^2(2+\cos\theta)]^{-\frac{2}{3}} \tag{28}$$

follows:

$$E(\theta,\theta_0) = (\pi\sigma_{lv}(\frac{3V}{\pi})^{\frac{2}{3}}) \cdot F \cdot [2 - 2\cos\theta - \Phi\sin^2\theta] \tag{29}$$

If we use:

$$\frac{E}{\pi\sigma_{lv}(\frac{3V}{\pi})^{\frac{2}{3}}} = \frac{G - A_{tot}\sigma_{sv}}{\pi\sigma_{lv}(\frac{3V}{\pi})^{\frac{2}{3}}} = E^{\star} \tag{30}$$

one can calculate the normed energy $E^{\star}$ which is no more dependent on the droplet volume and liquid surface tension:

$$E^{\star}(\theta,\theta_0) = [(1-\cos\theta)^2(2+\cos\theta)]^{-\frac{2}{3}}(2 - 2\cos\theta - \cos\theta_0\sin^2\theta) = F[2 - 2\cos\theta - \Phi\sin^2\theta] \tag{31}$$

For calculations we wrote a computer-code in MATLAB. The left-image of Fig. 3 depicts the energy surface in dependence of the material surface chemistry (intrinsic contact angle) and the contact angle imposed artificially by the calculation code.
The right-panels of Fig. 3 presents the path of minimal energy (upper panel) obtained from the energy map. The contact angles corresponding to the path of minimal energy is given

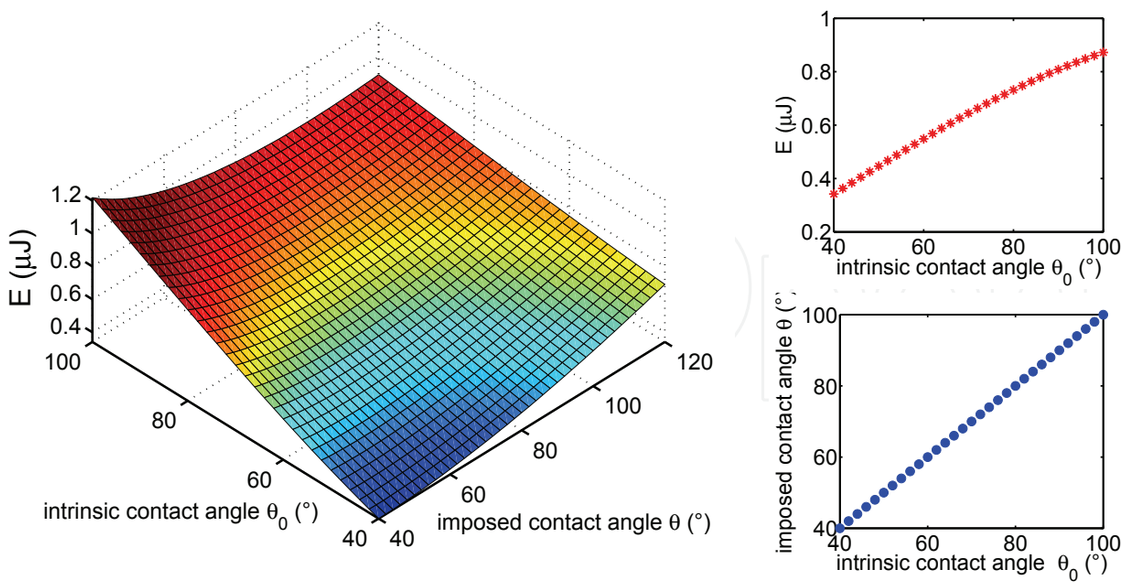

Fig. 3. Left-image: Energy map of a liquid droplet on flat surfaces with changing surface chemistry (intrinsic contact angle). Right upper panel: Path of minimal energy obtained from the left energy map. Right lower panel: The contact angles corresponding to the path of minimal energy. Drop volume $5\mu L$.

in the lower panel. It can be observed that equilibrium contact angles equals the intrinsic contact angles. This can be obtained also by the differentation of eq. (26) after θ and finding the minima by setting the diferential equal with zero:

$$0 = \frac{\partial E(\theta,\theta_0)}{\partial\theta} \Longleftrightarrow 0 = \frac{\partial E^{\star}(\theta,\theta_0)}{\partial\theta} = \frac{\partial[F(\theta)\cdot(2-2\cos\theta-\Phi(\theta_0)\sin^2\theta)]}{\partial\theta} =$$

$$\left(\frac{\partial F}{\partial\theta}\right)\cdot(2-2\cos\theta-\Phi\sin^2\theta)+F\cdot\left(\frac{\partial(2-2\cos\theta-\Phi\sin^2\theta)}{\partial\theta}\right)=[(1-\cos\theta)^2(2+\cos\theta)]^{-\frac{5}{3}}$$

$$\cdot(\sin\theta)\cdot[-2\sin^2\theta+2\cos\theta\sin\theta+2-3\cos\theta+\cos^3\theta-\Phi(\cos^4\theta-\sin^4\theta+2\cos\theta-3\cos^2\theta)] \quad (32)$$

There are three factors in the last expression of eq.(32). The first factor possesses a negative exponent which requires that:

$$(1-\cos\theta)^2(2+\cos\theta)\neq 0 \Longrightarrow \theta\neq 2n\pi \quad (33)$$

The second factor is $(\sin\theta)$. Considering the restriction (33), $\sin\theta$ vanishes for:

$$\theta = (2n+1)\pi \quad (34)$$

For $\theta=(2n+1)\pi$ the drop is entirely surrounded by the fluid and corresponds to an extrema, but which is a maxima instead of a minima. So, the vanishing of the last multiplier of the Gibbs-energy derivative (32) should furnish the energy minima:

$$-2\sin^2\theta+2\cos\theta\sin\theta+2-3\cos\theta+\cos^3\theta-\Phi(\cos^4\theta-\sin^4\theta+2\cos\theta-3\cos^2\theta)=0 \quad (35)$$

Equation (35) leads to:

$$\Phi=\frac{-2\sin^2\theta+2\cos\theta\sin\theta+2-3\cos\theta+\cos^3\theta}{\cos^4\theta-\sin^4\theta+2\cos\theta-3\cos^2\theta}\Rightarrow$$

$$\Phi=\frac{(-\cos\theta)(1-\cos\theta)^2}{-(1-\cos\theta)^2}\Longrightarrow\Phi=\cos\theta \quad\Longleftrightarrow\quad \cos\theta=\Phi \quad (36)$$

For smooth surfaces follows:

$$\cos\theta^{equil}=\cos\theta_0=\Phi=\Phi_{smooth} \quad (37)$$

Equation (36) is an important expression which will find discussion also in the following sections. The next section investigates the influence of gravity on the equilibrium state.

4.2 Gravity contribution included

If we insert eq. (18) in eq. (29) one obtains the energy of the system with the gravity contribution included:

$$E(\theta,\theta_0) = (\pi\sigma_{lv}(\frac{3V}{\pi})^{\frac{2}{3}})F[2-2\cos\theta-\Phi\sin^2\theta] + \frac{(3^{\frac{1}{3}})\rho(V^{\frac{4}{3}})g}{4\pi^{\frac{1}{3}}}\cdot\frac{(1-\cos\theta)^{\frac{1}{3}}(3+\cos\theta)}{(2+\cos\theta)^{\frac{4}{3}}} \quad (38)$$

The contact-angles corresponding to the minimization of the Gibbs energy minima are obtained by:

$$0 = \frac{\partial E(\theta,\theta_0)}{\partial\theta} \Longleftrightarrow$$

$$0 = \frac{\partial\left[(\pi\sigma_{lv}(\frac{3V}{\pi})^{\frac{2}{3}})\cdot F(\theta)\cdot(2-2\cos\theta-\Phi\sin^2\theta)\right]}{\partial\theta} + \frac{\partial\left[\frac{(3^{\frac{1}{3}})\rho(V^{\frac{4}{3}})g}{4\pi^{\frac{1}{3}}}\cdot\frac{(1-\cos\theta)^{\frac{1}{3}}(3+\cos\theta)}{(2+\cos\theta)^{\frac{4}{3}}}\right]}{\partial\theta} \quad (39)$$

According to eqs. (32,35,36) the first term in eq. (39) can be written as:

$$\frac{\partial\left[(\pi\sigma_{lv}(\frac{3V}{\pi})^{\frac{2}{3}})\cdot F(\theta)\cdot(2-2\cos\theta-\Phi\sin^2\theta)\right]}{\partial\theta} =$$

$$= (\pi\sigma_{lv}(\frac{3V}{\pi})^{\frac{2}{3}})\cdot[(1-\cos\theta)^2(2+\cos\theta)]^{-\frac{5}{3}}\cdot(\sin\theta)\cdot(1-\cos\theta)^2\cdot(-\cos\theta-\Phi) \quad (40)$$

The second term of eq. (39):

$$\frac{\partial\left[\frac{(3^{\frac{1}{3}})\rho(V^{\frac{4}{3}})g}{4\pi^{\frac{1}{3}}}\cdot\frac{(1-\cos\theta)^{\frac{1}{3}}(3+\cos\theta)}{(2+\cos\theta)^{\frac{4}{3}}}\right]}{\partial\theta} =$$

$$(\frac{(3^{\frac{1}{3}})\rho(V^{\frac{4}{3}})g}{4\pi^{\frac{1}{3}}}\cdot[(1-\cos\theta)^2(2+\cos\theta)]^{-\frac{5}{3}}\cdot(\sin\theta)\cdot(1-\cos\theta)^2\cdot\frac{(1-\cos\theta)^{\frac{2}{3}}}{(2+\cos\theta)^{-\frac{1}{3}}} \quad (41)$$

Inserting eqs. (40) and (41) into eq. (39) one obtains the contact angles which corresponds to the Gibbs energy minima by solving the equation:

$$V^2\rho^3g^3(1-\cos\theta)^2 = 3\pi^2\sigma_{lv}^3(2+\cos\theta)(\cos\theta+\Phi)^3 \quad (42)$$

Hence, the contact angles (θ^{equil}) corresponding to the Gibbs energy minima are a function of the drop-volume (V), liquid-density (ρ), liquid-fluid surface tension (σ_{lv}) and (Φ).
Without gravitational contribution, an analytical solution can be easily achieved because eq. (37) is simple. Including the gravity field, the equation becomes of fourth order (eq. (42)). A analytical solution is possible, but more difficult. A numerical solution of eq. (42) is more convenient.
In our laboratory the volume of the water drop usualy used to measure contact angles was 5 μL. As mentioned in the previous section, the minimal volume of the droplet considered in this work should be 0.4 μL. Maximum droplets can be considered possessing a radius

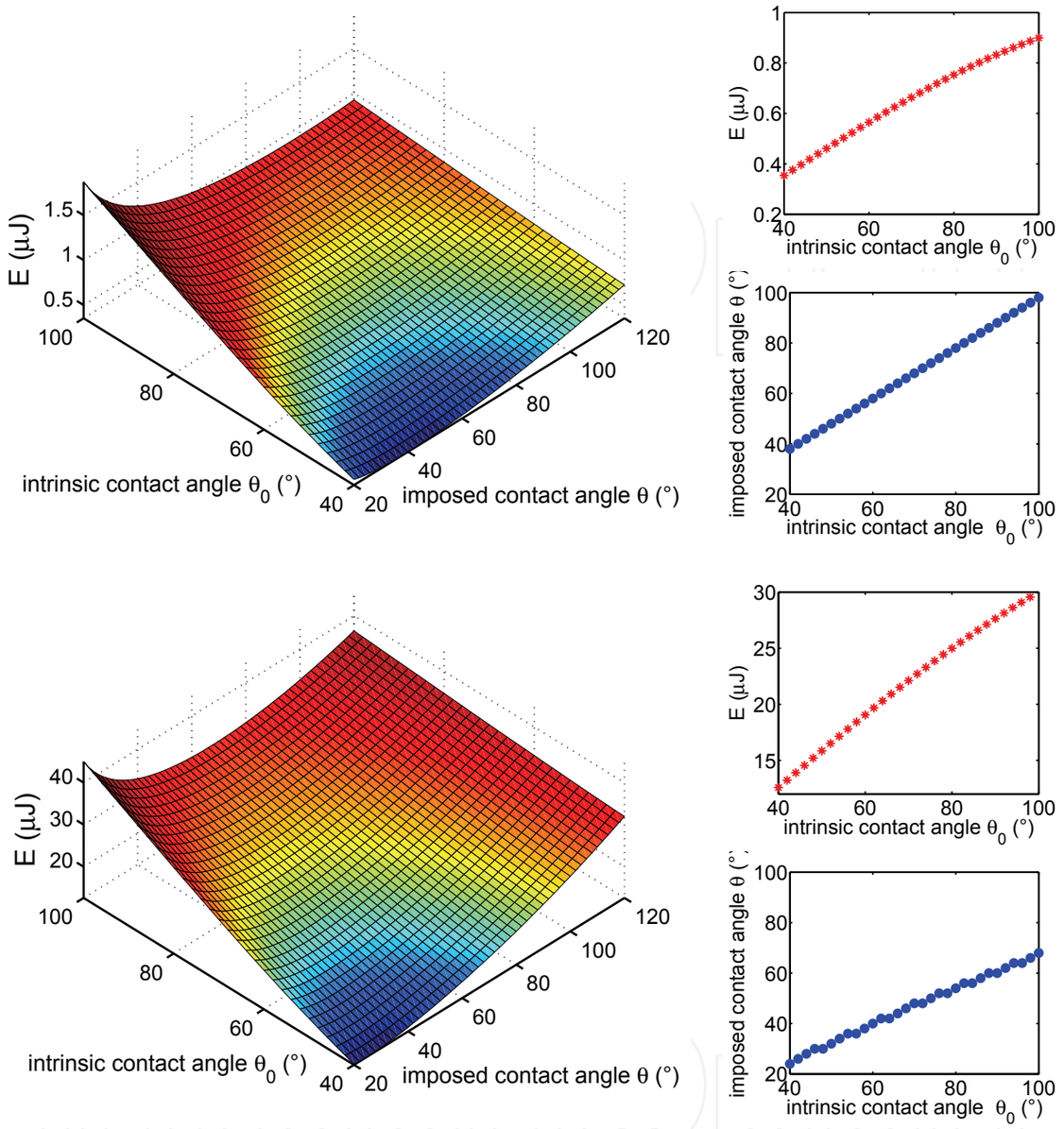

Fig. 4. Effect of gravitational field on a liquid droplet resting on a flat surface. Left images: energy maps in dependence of the surface chemistry (intrinsic contact angle) and the drop contact angle imposed by the calculation code. Gravity contribution is included for drop volumes of 5 μL (upper panel) and 523 μL (lower panel). Right panels: Path of minimal energy and corresponding contact angles of the energy surfaces depicted in the left-images.

of 5 mm, having in that way a volume of 523 μL. With $g = 9.81 m/s^2$, $\rho = 1000 kg/m^3$ and $\sigma_{lv} = 0.072 N/m$ one obtains the energy maps illustrated in the left images of Fig. 4 for water drop volumes of 5 μL (upper panel) and 523 μL (lower panel).
The corresponding paths of minimal energy and the equilibrium contact angles are presented in the right panels of Figure 4. The gravity contribution increase the energy of each state. Large

drops changes the topography of the energy map. Small drops do not change the equilibrium state whereas large drops can reduce significantly the equilibrium contact angle.
In the case a drop is hanging from (instead of resting on) a surface, the gravity contribution has to be subtracted from (instead of adding to) the Gibbs energy:

$$E(\theta,\theta_0) = (\pi\sigma_{lv}(\frac{3V}{\pi})^{\frac{2}{3}})F[2-2\cos\theta-\Phi\sin^2\theta] - \frac{(3^{\frac{1}{3}})\rho(V^{\frac{4}{3}})g}{4\pi^{\frac{1}{3}}}\cdot\frac{(1-\cos\theta)^{\frac{1}{3}}(3+\cos\theta)}{(2+\cos\theta)^{\frac{4}{3}}} \quad (43)$$

With $g = 9.81m/s^2$, $\rho = 1000kg/m^3$ and $\sigma_{lv} = 0.072N/m$ one obtains the energy maps depicted in the left images of Fig. 5 for water drops hanging from a surface for droplet volumes of 5 μL (upper panel) and 523 μL (lower panel).
The right panels of Fig. 5 presents the path of minimal energy and the corresponding equilibrium contact angles. The gravity contribution reduces the energy of each state. The topography of the energy map is strongly influenced for large drops. Small drops do not change the equilibrium state whereas large drops enhance significantly the equilibrium contact angle. Equilibrium contact angles approaching 180 degrees reflect drops which lost contact to surface. As the lowest panel of Fig. 5 shows, the equilibrium contact angle for large drops jumps to 180 degrees also for water-attractive surface chemistries (hydrophilic materials). In general, for drops hanging from the surface, the gravity contribution acts alike a non-adhesive (repulsive) field, whereas for drops resting on surfaces the gravity acts alike an adhesive field.
Figure 6 shows the path of minimal energy and Fig. 7 the corresponding equilibrium contact angles as a function of the drop volume and the surface chemistry for drops resting (left panels) and hanging (right panels) from smooth surfaces.
The next section investigates the case of rough surfaces.

5. Full-wetted rough surfaces. Wenzel regime.

This chapter analyses the case where rough surfaces beneath the drop-base are fully wetted. Textured surfaces with roughness-features smaller than the size of the drop-base will be considered.

5.1 Without gravity contribution

The area of the solid-liquid interface is given by:

$$A_{sl} = r\cdot A_{drop-base} = r\cdot\pi(R_0\sin\theta)^2 \quad (44)$$

where r is the roughness ratio defined as the fraction between the real and projected surface. The roughness parameter r is always larger than unity. It equals 1 for flat surfaces.
The vapor-liquid interface remains the same as given in eq. (20). Introducing eq. (44) into the formula of the Gibbs-energy eq. (6) one obtains with the help of eqs. (10), (29) and (28):

$$E(\theta,\theta_0,r) = (\pi\sigma_{lv}(\frac{3V}{\pi})^{\frac{2}{3}})F[2-2\cos\theta-r(\cos\theta_0)\sin^2\theta] \quad (45)$$

The normed energy $E^\star$ is then given by:

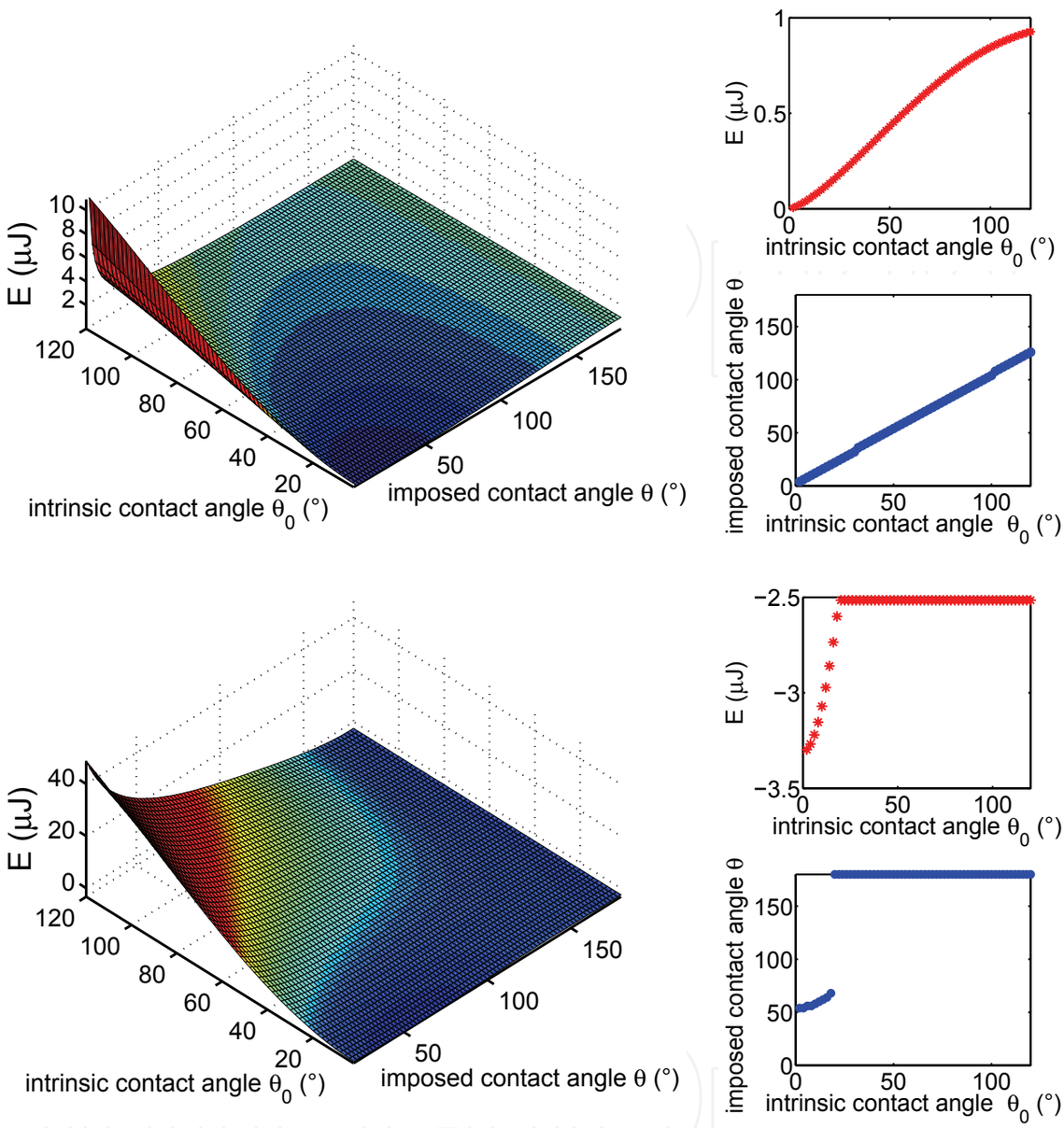

Fig. 5. Effect of gravitational field on a liquid droplet hanging from a flat surface. Left images: energy maps in dependence of the surface chemistry (intrinsic contact angle) and the drop contact angle imposed by the calculation code. Gravity contribution is included for drop volumes of 5 μL (upper panel) and 523 μL (lower panel). Right panels: Path of minimal energy and corresponding contact angles of the energy surfaces depicted in the left-images.

$$E^{\star}(\theta,\theta_0,r) = F(\theta)\cdot[2-2\cos\theta - r\cdot(\cos\theta_0)\sin^2\theta] \tag{46}$$

By comparing eq. (29) with eq. (45) one obtains:

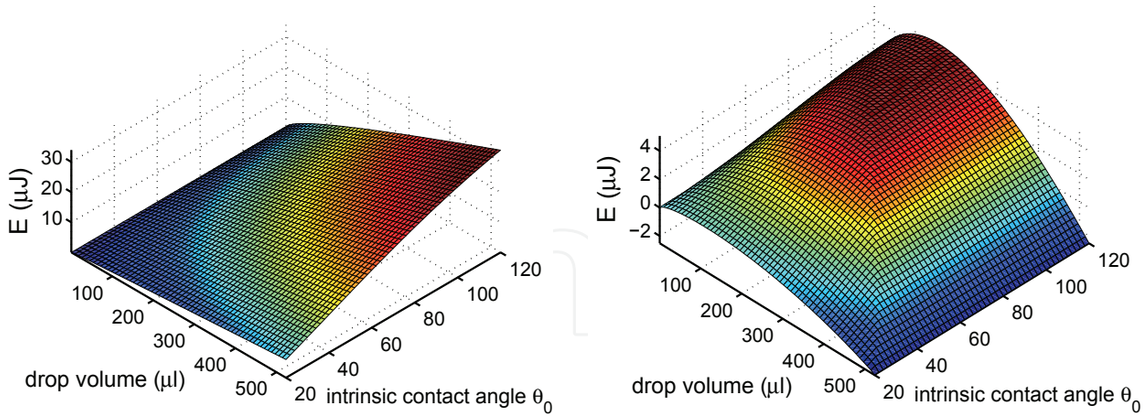

Fig. 6. Energy minima map of a liquid droplet resting on (left panel) or hanging from (right panel) a flat surface as a function of the drop volume and the surface chemistry (expressed by intrinsic contact angle), with gravity contribution included.

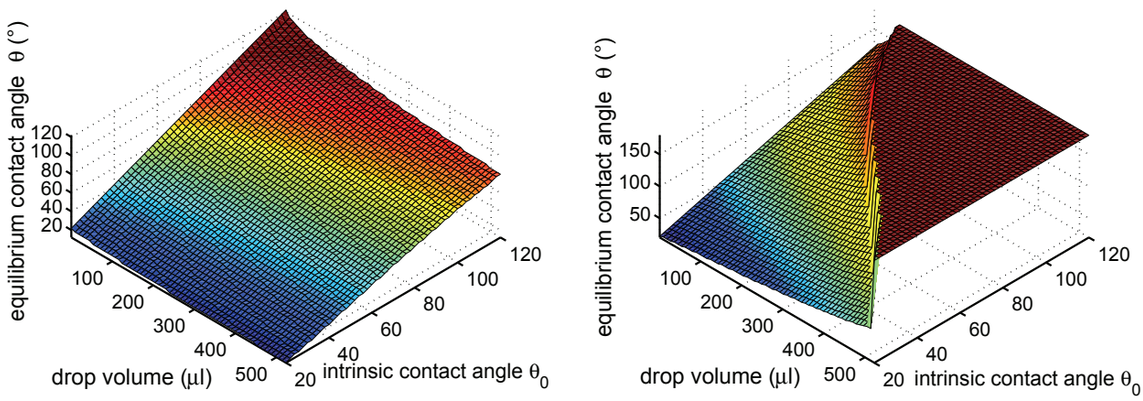

Fig. 7. Equilibrium contact angles of a liquid droplet resting on (left panel) or hanging from (right panel) a flat surface as a function of the drop volume and the surface chemistry (expressed by intrinsic contact angle), with gravity contribution included. $\theta \cong 180^o$ means that the drop lost his contact to surface. This is the case for large drops hanging from the surface.

$$\Phi(\theta_0) = \Phi_{rough}(\theta_0) = r \cdot \cos\theta_0 \tag{47}$$

From the solution (eq. (37)) of energy minimization (eq. (32)) one obtains the equillibrium contact angle of the drop on the rough surface given by:

$$\cos\theta = r \cdot \cos\theta_0 = \Phi = \Phi_{rough} \tag{48}$$

Equation (48) is the well-known Wenzel equation which provides the contact angle of a drop on a rough surface if on the drop-base the surface is fully wetted. For the case of the *Colocasia esculenta* leaf presented in Fig. 2 the roughness parameter r is 2.60. The left image of Fig. 8

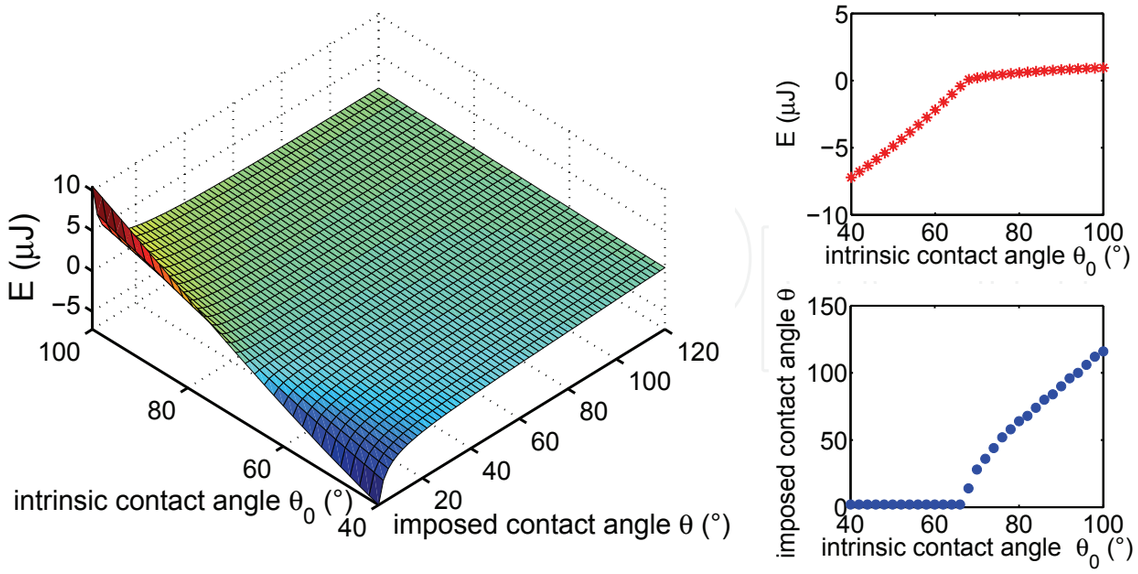

Fig. 8. Left-image: Energy map of a liquid droplet on the rough surfaces of the *Colocasia esculenta* leaf, in dependence of surface chemistry (intrinsic contact angle) and drop contact angle. Right panels: Path of minimal energy obtained from the left energy map. Corresponding equilibrium contact-angles.

illustrates the energy surface E of a drop on the *Colocasia esculenta* leaf surface as a function of the material surface chemistry (intrinsic contact angle) and the contact angle imposed artificially by the calculation code.
The paths of minimal energy and equilibrium contact-angles are presented in the right-panels. It can be observed that equilibrium contact angles are given by the Wenzel equation (48).

5.2 Gravity contribution included

If we insert eq. (18) by adding or subtracting into eq. (45) one obtains the energy of the system for drops resting on a rough surface or hanging from a rough surface with the gravity contribution included:

$$E(\theta,\theta_0) = (\pi\sigma_{lv}(\frac{3V}{\pi})^{\frac{2}{3}})F[2-2\cos\theta-\Phi\sin^2\theta] \pm \frac{(3^{\frac{1}{3}})\rho(V^{\frac{4}{3}})g}{4\pi^{\frac{1}{3}}}\frac{(1-\cos\theta)^{\frac{1}{3}}(3+\cos\theta)}{(2+\cos\theta)^{\frac{4}{3}}} \quad (49)$$

Figure 9 presents the path of minimal energy and Fig. 10 the corresponding equilibrium contact angles as a function of the drop volume and the surface chemistry. Again, for drops hanging from the surface the gravity contribution act alike a non-adhesive (repulsive) field, whereas for drops resting on surfaces it acts alike an adhesive field.
The next section shows the energy and the equilibrium contact angles for all drop states appeared during the drop-sink into the surface roughness.

6. Partial-wetting: Cassie-Baxter

Partially wetted states have the wetting-fraction in between 0 und 1 ($0 < f < 1$). For $f = 1$ the state is defined as wetted (or Wenzel state) where on the drop-base the material surface

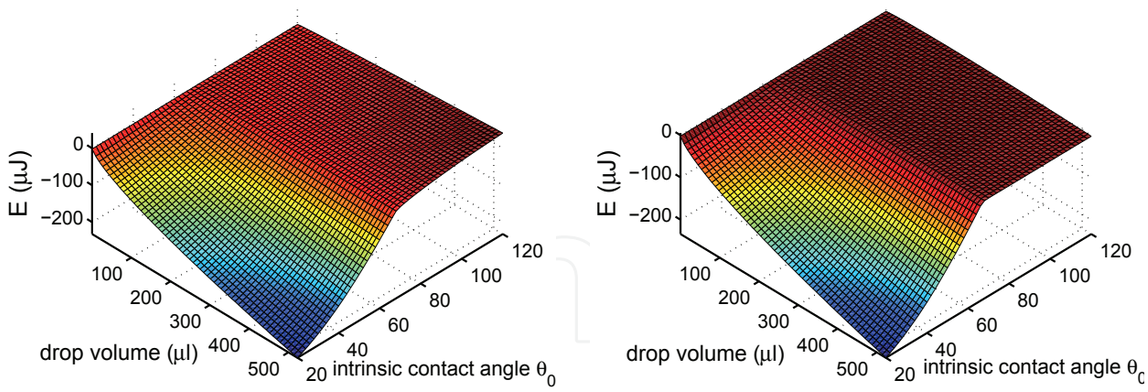

Fig. 9. Wetting regime: Energy minima map of a liquid droplet resting on (left panel) or hanging from (right panel) the surface of *Colocasia esculenta* leaf as a function of the drop volume and the surface chemistry (expressed by intrinsic contact angle), with gravity contribution included.

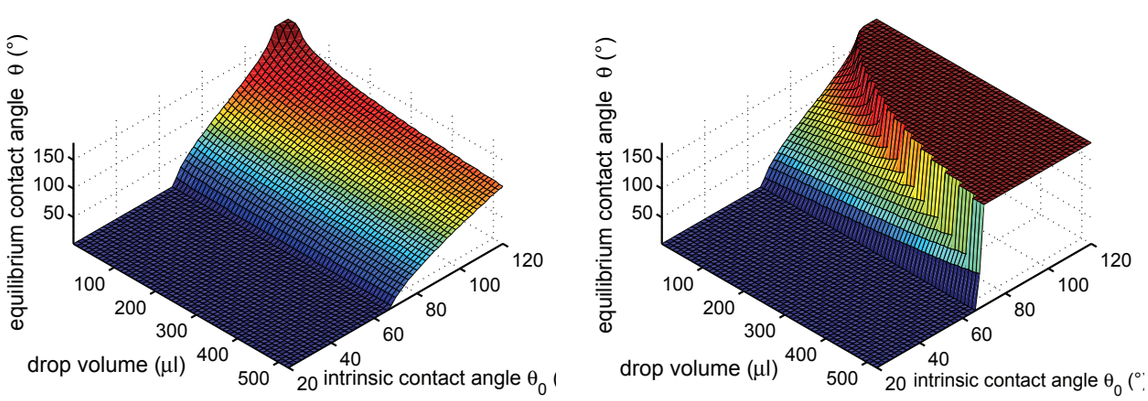

Fig. 10. Wetting regime: Equilibrium contact angles of a liquid droplet resting on (left panel) or hanging from (right panel) the surface of *Colocasia esculenta* leaf as a function of the drop volume and the surface chemistry (expressed by intrinsic contact angle), with gravity contribution included. $\theta \cong 180^o$ means lack of contact to surface, i.e. drop is falling.

is fully wetted. States for which $f = 0$ will be defined as non-bonded states. Drops hanging with $f = 0$ are falling.

The main objective of this subsection is to investigate the existence of Gibbs energy minima for states where underneath the drop-base the material surface is only partial wetted, i.e. if energy minima appears during the drop's sink into the surface roughness. This appears if there is an energy barrier between the wetting (Wenzel) state and the partial wetting (Cassie-Baxter) state. Obviously, such a energy barrier cannot be produced by a flat surface.

In the following we make the assumption that the water-front on the drop-base which sinks into the surface roughness is allways parallel to the macroscopic surface, as sketched in Fig. 2. The area of the solid-liquid interface is then given by:

$$A_{sl}(x) = r(x) \cdot f(x) \cdot A_{drop-base} = r(x) \cdot f(x) \cdot \pi (R_0 \sin\theta)^2 \tag{50}$$

where $x = z/zmax$ is the sink depth ratio between the intermediate (z) and maximal (zmax) sink depth. The sink depth ratio x is in between 0 and 1. It is equal to 0 for the case the drop do not sink into the surface roughness and is equal to 1 if on the drop base all the surface is wetted. $f(x)$ is the fraction of the flat drop-base area which is wetted at the sink depth ratio x. Obviously also the roughness ratio is a function of the sink depth ratio $r = r(x)$.
Usually, surfaces possess one roughness-ratio (r) and one wetting-fraction (f) at a given sink-depth ratio (x). Hence, in place of expressing r and f by the sink-depth, one can directly express the roughness-ratio as a function of the wetting-fraction ($r(f)$). Figure 11 illustrates the wetted area of the papillae of *Colocasia esculenta* leaf for four sink-depths (i.e. four wetting fractions). The drop base is considered to be larger than the extent of the AFM images. The flat white regions in between the roughness corresponds to the non-wetted $(1-f)$ part of the drop-base, i.e. the liquid-vapor interface on the drop-base. Figure 12 presents the dependence of the roughness ratio (r) on the wetting fraction (f) for the papillae of *Colocasia esculenta* leaf. With the help of this surface morphology characteristics we will compute the Gibbs energy in dependence of the surface chemistry. The results are presented in the following subsections.

6.1 Without gravity contribution

The area of the liquid-vapor interface is given by adding to eq. (20) also the non-wetted part of the drop-base area $(1-f)\pi(R_0\sin\theta)^2$:

$$A_{lv} = \pi R_0^2(2-2\cos\theta) + (1-f(x))\cdot\pi(R_0\sin\theta)^2 \tag{51}$$

By introducing the eqs. (50) and (51) into the formula of the Gibbs-energy eq. (6) one obtains with the help of eqs. (10), (25) and (28):

$$G^\star(\theta,\theta_0,x) = F(\theta)\cdot[2-2\cos\theta-(r\cdot f\cdot\cos\theta_0-1+f)\sin^2\theta] \tag{52}$$

where the wetted fraction f and the roughness ratio r are functions of the sink depth ratio x.
From the solution (eq. (37)) of energy minimization (eq. (32)) one obtains the equilibrium contact angle of the drop on the rough surface given by:

$$\cos\theta^{equil} = r\cdot f\cdot\cos\theta_0 + 1 - f = \Phi \tag{53}$$

This equation is the well-known Cassie-Baxter equation which provides the contact angle of the drop in different partial wetting states. For $x = 0$ one have $f = 0$ from which follows that $\theta = 180^o$. For full wetting on the drop-base ($f = 1$) the Cassie-Baxter equation (53) transforms into the Wenzel equation (48) which describes the wetting regime.
The Cassie-Baxter equation (eq. (53)) does not predict if there exists a stable or metastable partial wetted state. Their existence is given by zero-points in the Gibbs energy derivatives after the sink-depth ratio:

$$0 = \frac{\partial G^\star(\theta,\theta_0,x)}{\partial x} \Longrightarrow 0 = \frac{\partial\Phi}{\partial x} = \frac{\partial(rf\cos\theta_0+1-f)}{\partial x} = \quad (r\frac{\partial f}{\partial x} + f\frac{\partial r}{\partial x})\cos\theta_0 - \frac{\partial f}{\partial x} \tag{54}$$

As can be observed from eq. (54), the sink-depths which corresponds to Gibbs energy extrema, depends on the surface chemistry (expressed by θ_o) and the surface roughness gradient (i.e. $\frac{\partial f}{\partial x}$ and $\frac{\partial r}{\partial x}$).

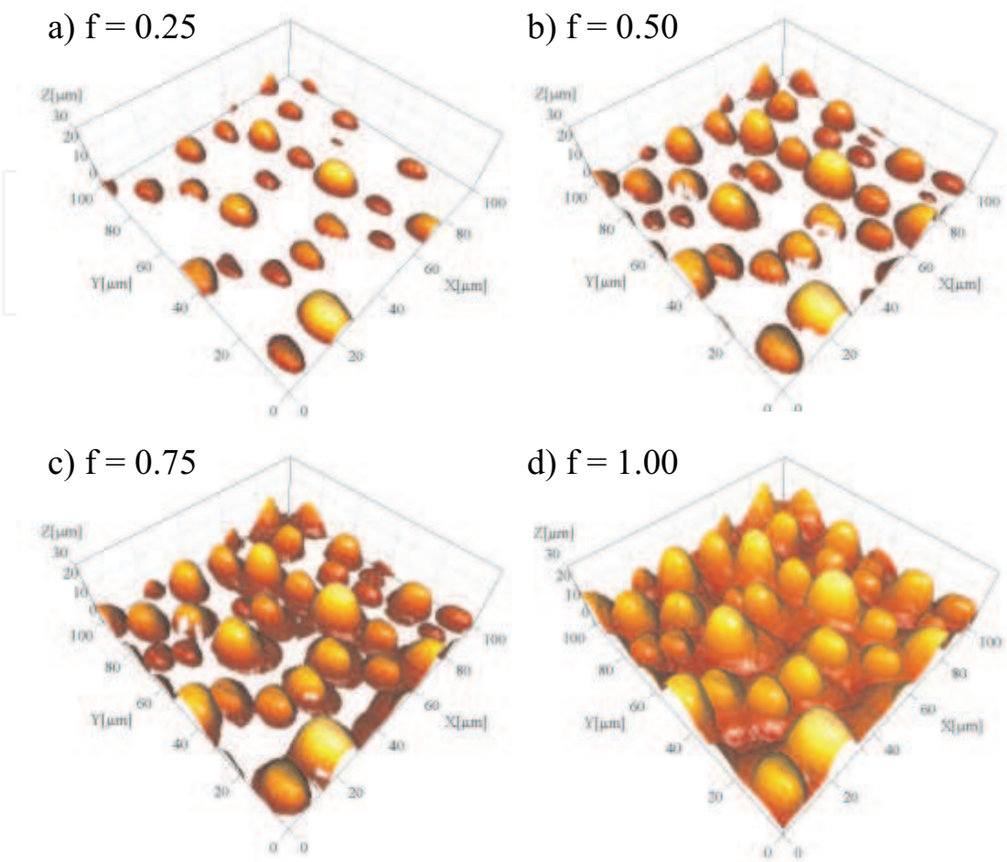

Fig. 11. The wetted area of *Colocasia esculenta* leaf surface roughness as a function of the wetting fraction f (i.e. as a function of the sink-depth). The pictures where obtained by processing with SPIP an atomic force microscopy image recorded from the *Colocasia esculenta* leaf. The wetted area of *Colocasia esculenta* for partial wetting f=0.25; 0.50; 0.75 and full-wetting f=1 are illustrated in the upper-left image (f=0.25), upper-right image (f=0.50), low-left image (f=0.75) and low-right image (f=1), respectively.

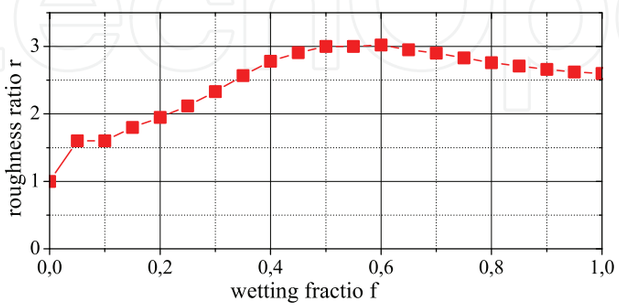

Fig. 12. Roughness ratio vs wetting fractio determined from the AFM image of *Colocasia esculenta* leaf.

In order to get the contact angles and sink-depths corresponding to Gibbs-energy minima, one can analytically solve the eqs. (54) and (53), or, alternatively, compute the Gibbs-energy for all possible contact angles (θ), all sink-depths (x) for a given surface morphology (f, r) and chemistry (θ_o): $G^\star = G^\star(\theta, \theta_0, r, f, x)$.
The second strategy is more convenient, especially, as previosly mentioned, when the gravity contribution is considered. Furtheremore, an analytical expression for f and r is not always easy to be determined, especially for random rough surfaces. Random rough surfaces are much more relevant from a practical perspective, because they are cheaper to fabricate. They can be made from a large class of materials, metallic and non-metallic. So, there is also a practical standpoint for the preference to compute the Gibbs energy for all possible contact angles, if random rough surfaces are considered.
Figure 13 presents the normed energy for a drop resting on papillaes of *Colocasia esculenta*. θ is the contact angle imposed artificially by the calculation code. For each wetting fraction f one can obtain the Gibbs energy minima and the corresponding (equilibrium) contact angle presented in Fig. 14 for intrinsic contact angles of $\theta_0 = 72^o$ (left panel), $\theta_0 = 109^o$ (middle panel) and $\theta_0 = 112^o$ (right panel).
For hydrophilic surface chemistry, Gibbs energy minima appears only in the wetted state ($f = 1$) (see Figs. 13,14). There is no energy barrier which could stop the wetting on the drop-base. So, for hydrophilic surface chemistry, always the wetting regime is obtained. This is different for hydrophobic surface chemistry. For hydrophobic surface chemistry, the *Colocasia esculenta* roughness induces a local Gibbs energy minima for partially-wetted states ($f < 1$) (Figs. 13,14). This can be observed also in Fig. 15 where the maps of the Gibbs energy minima and their corresponding maps of contact angles are presented in dependence of surface chemistry (θ_0) and wetting fraction. Firstly, for hydrophobic contact angles up to ($\theta_0 = 110^o$) the Gibbs energy minima for partial-wetting is metastable. The global minimum being the wetting-regime ($f = 1$). For intrinsic contact angles higher than 110^o, the partial-wetting generates the global minimum.
The stars surrounded by circles in Fig. 16 reveal that the partially-wetted states are global minima.

6.2 Gravity contribution included

If we insert eq. (18) in eq. (52) one obtains the energy of the system with the gravity contribution included for drops resting on (+) or hanging from (-) rough composite surfaces:

$$E(\theta, \theta_0) = (\pi\sigma_{lv}(\frac{3V}{\pi})^{\frac{2}{3}})F[2 - 2\cos\theta - \Phi\sin^2\theta] \pm \frac{(3^{\frac{1}{3}})\rho(V^{\frac{4}{3}})g}{4\pi^{\frac{1}{3}}} \cdot \frac{(1-\cos\theta)^{\frac{1}{3}}(3+\cos\theta)}{(2+\cos\theta)^{\frac{4}{3}}} \quad (55)$$

In order to investigate the gravity contribution on the wetting behavior, we compare the case of no-gravity inclusion with the case when the gravity contribution is included. This will be done for a drop volume 523 μL resting on or hanging from the *Colocasia esculenta* leaf.
With $g = 9.81 m/s^2$, $\rho = 1000 kg/m^3$ and $\sigma_{lv} = 0.072 N/m$ one obtains the energy maps illustrated in Fig. 17 for resting drops (middle row) and for hanging drops (lower raw). Figure 18 presents the path of energy minima in dependence of the wetting-fractio (f) for drops resting or hanging in the case of no-gravity contribution and the case of gravity contribution included. The corresponding contact angles are presented in Fig. 19.
Gravity enhance (reduce) the Gibbs energy for drops resting on (hanging from) surfaces. On that way, the gravity field reduces (enlarges) the contact angle of energy minima states, for

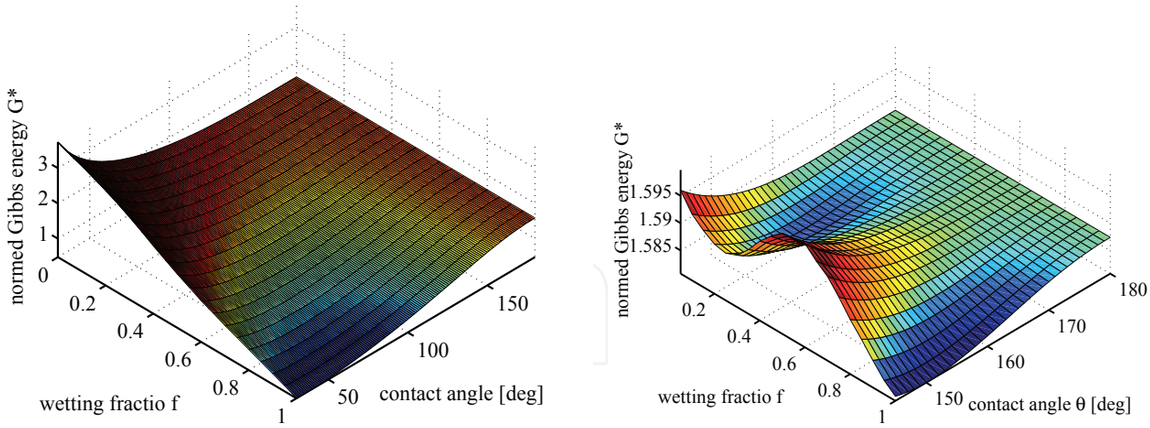

Fig. 13. *Colocasia esculenta* leaf: No gravity consideration. Normed Gibbs energy of a liquid droplet as a function of the wetting fraction f and the contact angle θ imposed artificially by the calculation code for a intrinsic contact angle of $\theta_0 = 72^o$ (left panel) and $\theta_0 = 109^o$ (right panel).

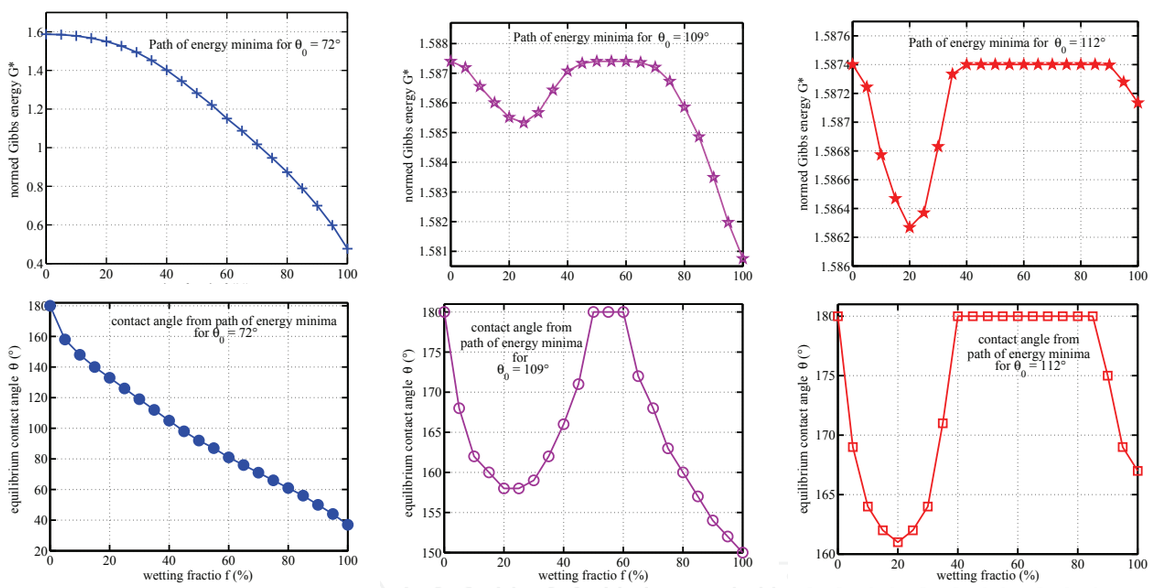

Fig. 14. *Colocasia esculenta* leaf: No gravity consideration. Upper row: Path of minimal Gibbs energy, e.g. obtained from the energy surface presented in Fig. 13 for intrinsic contact angle of $\theta_0 = 72^o$ (left panel), $\theta_0 = 109^o$ (middle panel) and $\theta_0 = 112^o$ (right panel). Lower row: The contact angles corresponding to the path of minimal energy.

drops resting on (hanging from) surfaces. Contact angles of $\theta = 180^o$ for hanging drops means drop-fall.

The dependence on the surface chemistry is presented in Fig. 20. Figure 21 presents the surface chemistry dependence of the Gibbs energy minima, their corresponding contact angles and the wetting fraction where the Gibbs energy minima appears.

The extension to liquids of different liquid surface tensions is straightforward. In that case σ_{lv} has to be changed. Of course, a different liquid yields the surface chemistry to establish a different intrinsic contact angle θ_0.

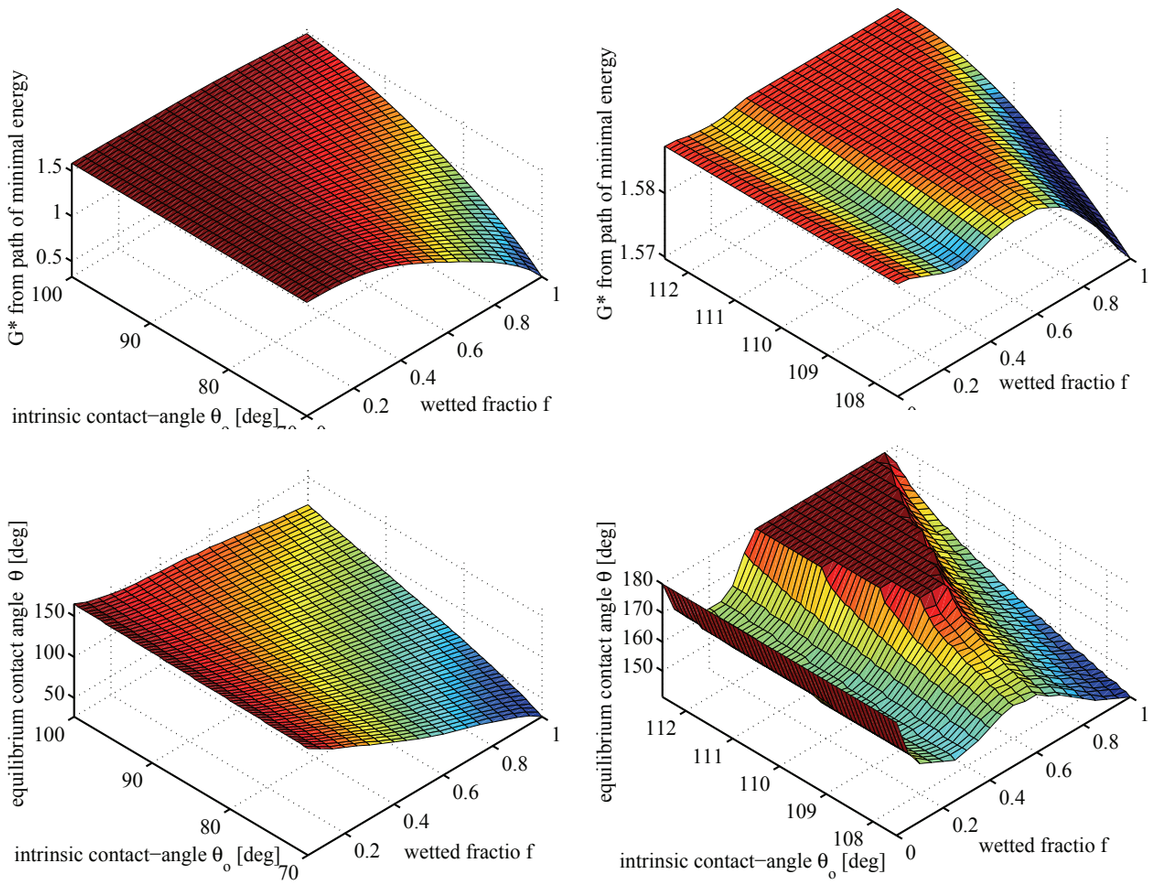

Fig. 15. *Colocasia esculenta* leaf: No gravity consideration. Upper row: Path of minimal Gibbs energy in dependence of the surface chemistry expressed by intrinsic contact angle of θ_0 (i.e. Gibbs energy minima as a function of wetting fraction and intrinsic contact angle). Lower row: The contact angles corresponding to the path of minimal energy.

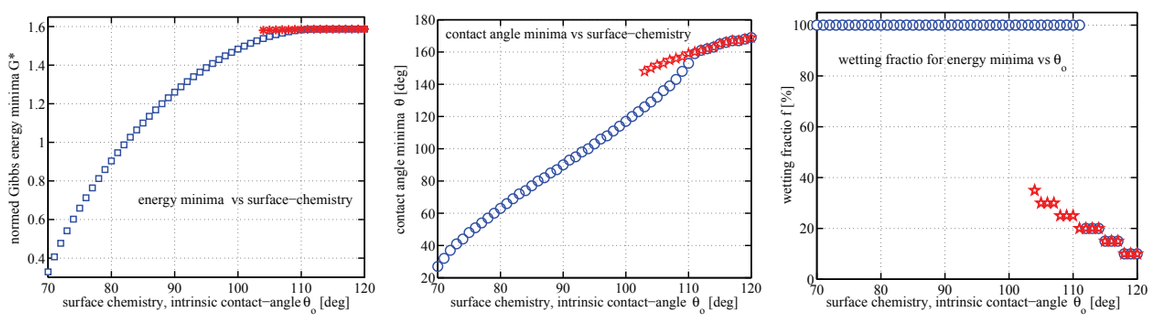

Fig. 16. *Colocasia esculenta* leaf: No gravity consideration. Left-panel: Metastable and global Gibbs energy minima in dependence of the surface chemistry expressed by the intrinsic contact angle. Stars mark partially-wetted states ($f < 1$). Circles denote the global minima. Stars surrounded by circles means that the partially-wetted states are global minima. Middle-panel: The contact angles corresponding to the Gibbs energy minima. Right-panel: The wetting fraction for the Gibbs energy minima.

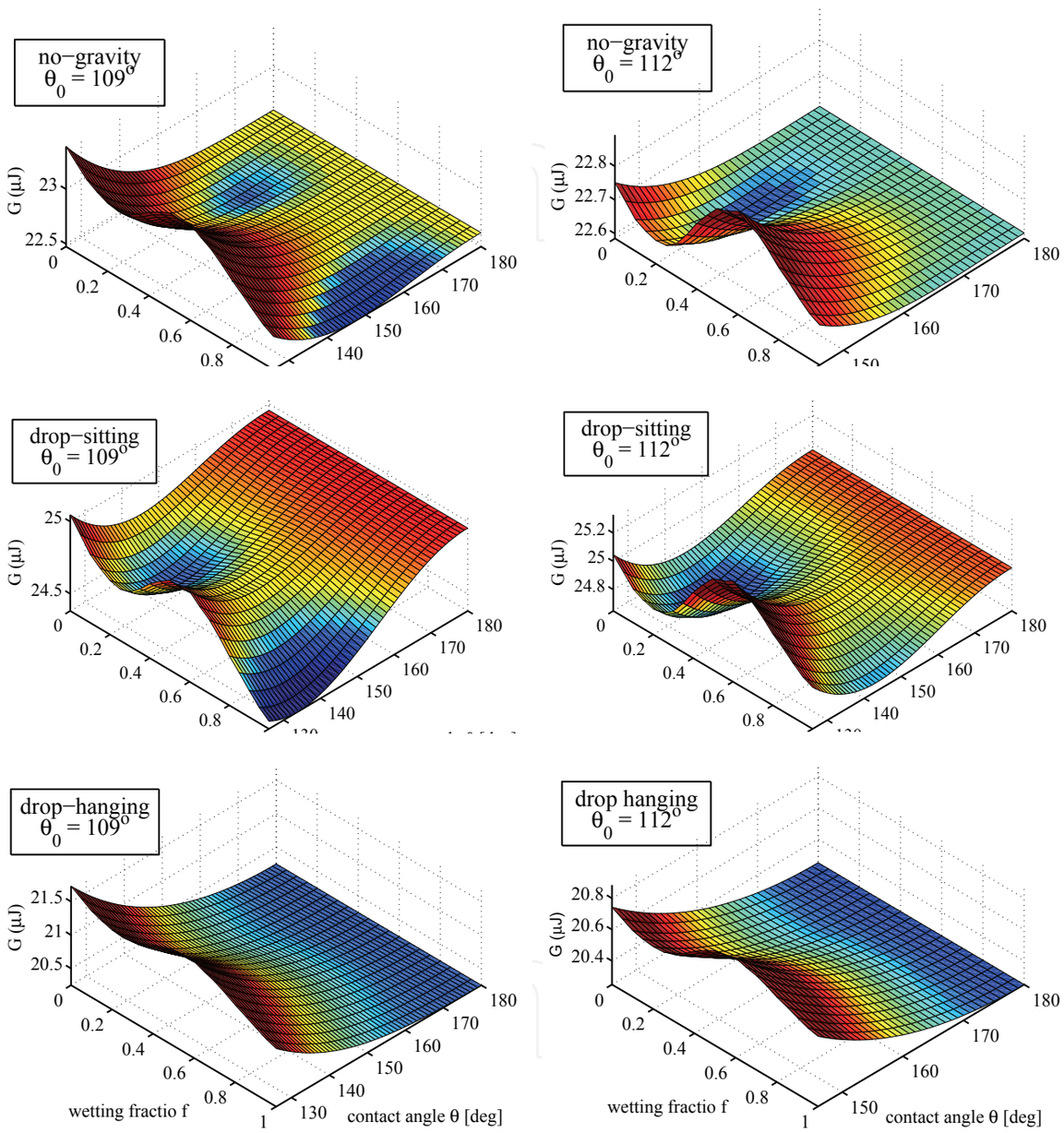

Fig. 17. *Colocasia esculenta* leaf: Effect of gravity for a drop resting (middle panels) or hanging (lower panels). Energy maps without (uppers panels) and with (middle and lower panels) gravity included as a function of the wetting fraction f and the contact angle θ imposed artificially by the calculation code. Left panels: for intrinsic contact angle of $\theta_0 = 109^o$. Right panels: $\theta_0 = 112^o$. The volume of the water droplet is 523 μL.

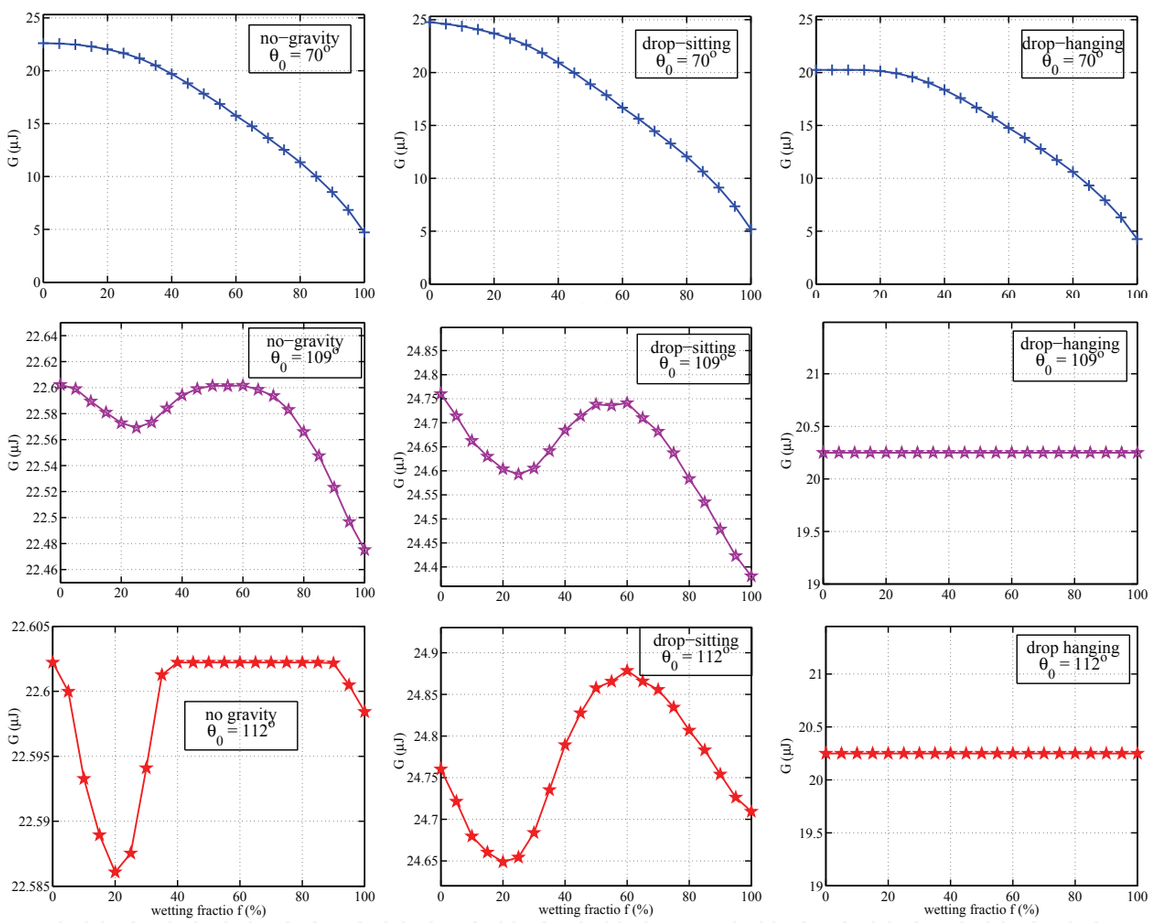

Fig. 18. *Colocasia esculenta* leaf: Effect of gravity on paths of minimal energy as a function of wetting fraction f. Paths of minimal Gibbs energy obtained from the energy surface presented in Fig. 17 with lack of gravity (left column), with gravity consideration for resting droplet (middle column) and with gravity contribution for hanging droplet (right column). Upper row: for intrinsic contact angle of $\theta_0 = 70^o$. Middle row: $\theta_0 = 109^o$. Lower row: $\theta_0 = 112^o$.

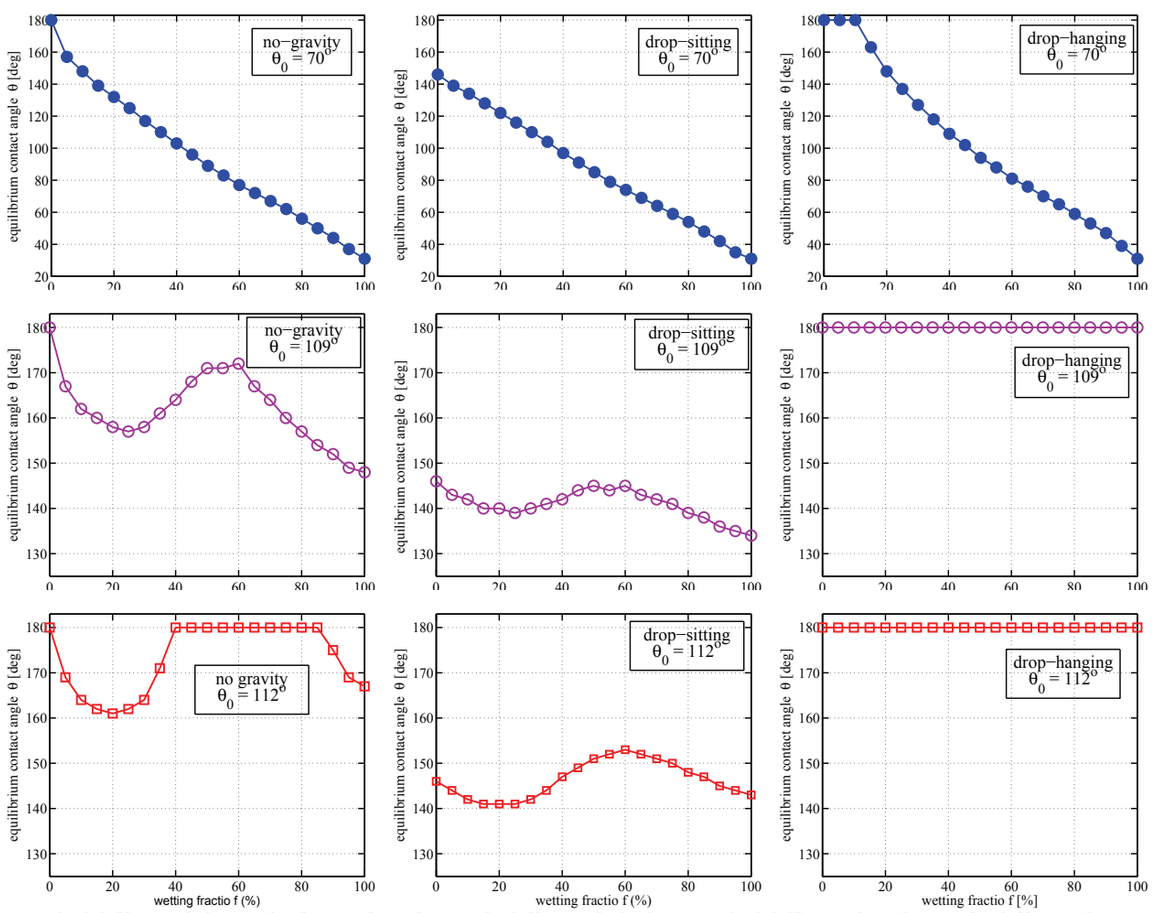

Fig. 19. *Colocasia esculenta* leaf: Effect of gravity on the contact angles corresponding to the paths of minimal energy as a function of wetting fraction f. Contact angles which corresponds to the paths of minimal Gibbs energy presented in Fig. 18. Lack of gravity (left column), with gravity consideration for resting droplet (middle column) and with gravity contribution for hanging droplet (right column). Upper row: for intrinsic contact angle of $\theta_0 = 70^o$. Middle row: $\theta_0 = 109^o$. Lower row: $\theta_0 = 112^o$.

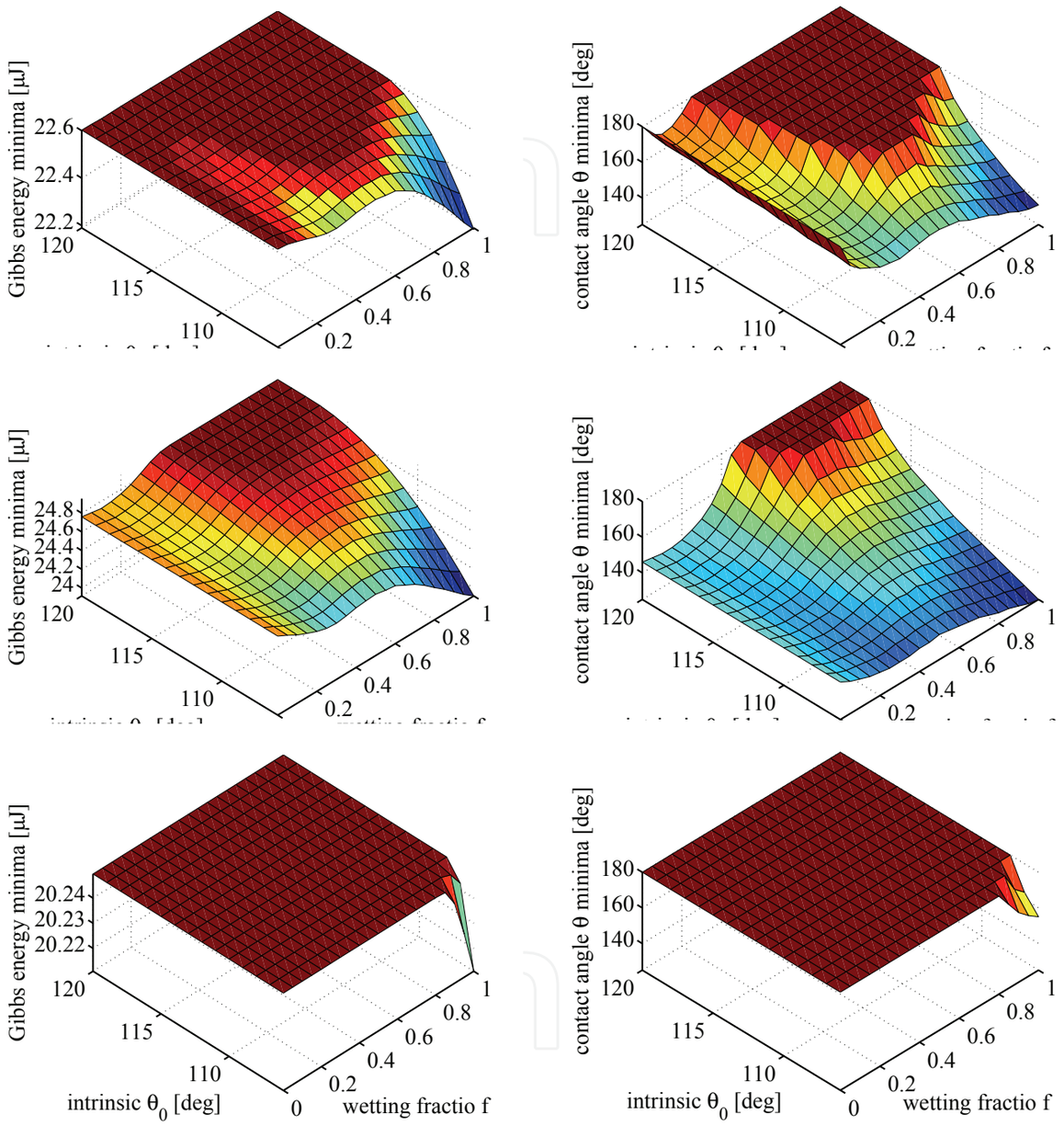

Fig. 20. *Colocasia esculenta* leaf: Effect of gravity on Gibbs energy minima (left panels) and their corresponding contact-angles (right panels) for drops resting (middle panels) or hanging as a function of the surface chemistry and wetting fraction. Upper panels: lack of gravity. Middle panels: gravity included for drop-resting. Lower panels: gravity included for drop-hanging.

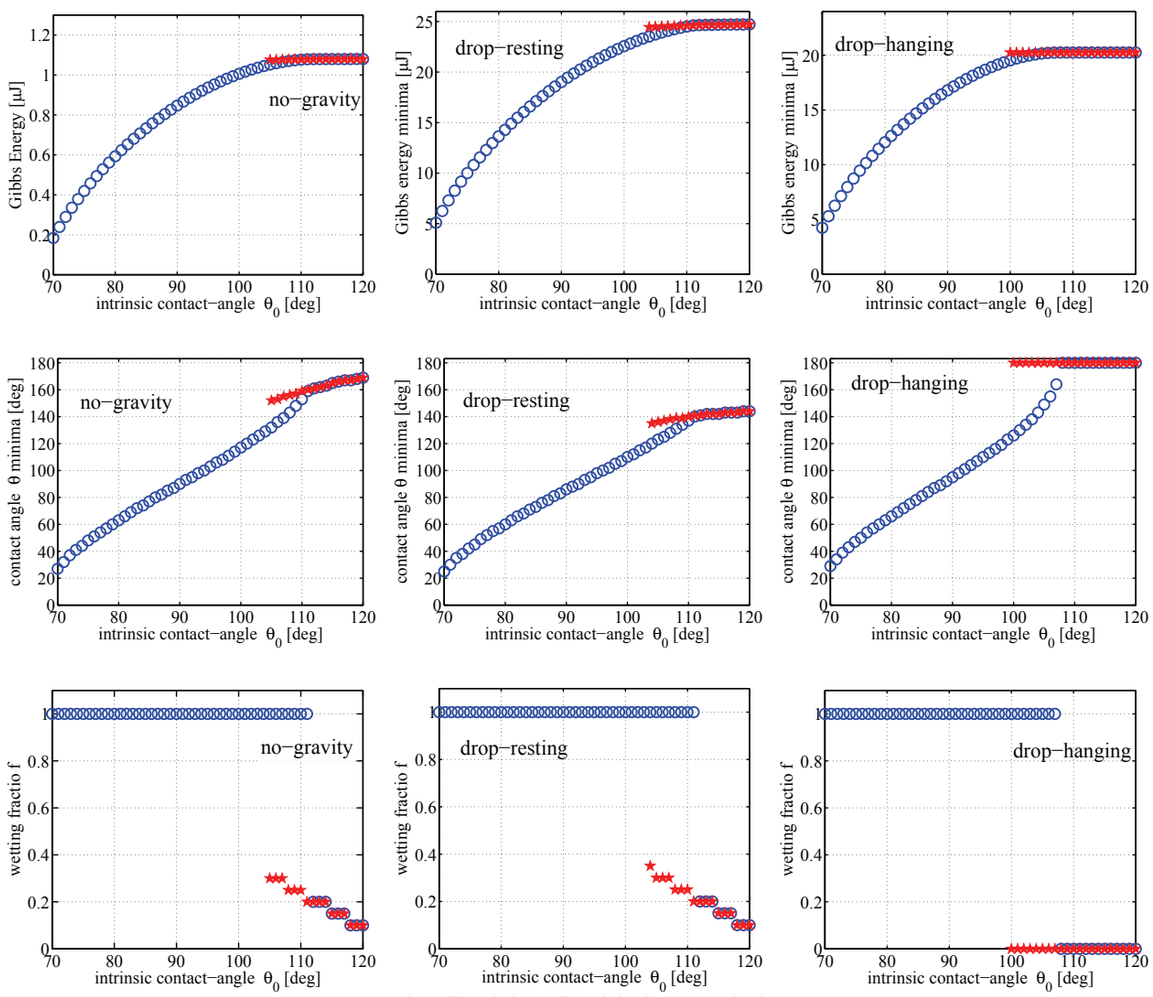

Fig. 21. *Colocasia esculenta* leaf: Effect of gravity on the values obtained for the paths of minimal energy as a function of the surface chemistry. Left-column: for no gravity. Middle-column: for drop resting. Right-column: for drop-hanging. Upper panels: Metastable and global Gibbs energy minima in dependence of the surface chemistry expressed by the intrinsic contact angle. Stars mark partially-wetted states ($f < 1$). Circles denotes the global minima. Stars surrounded by circles means that the partially-wetted states are global minima. Middle panels: The contact angles corresponding to the Gibbs energy minima. Lower panels: The wetting fraction for the Gibbs energy minima.

7. Conclusion and Outlook

We described an easy to handle Gibbs energy function to study the influence of surface chemistry and surface roughness on liquid wetting behaviour. An example how forces affect the wetting behavior was supplied by considering the gravitational field. The equations were applied on the surface morphology measured by atomic force microscopy from the evolution-optimized self-cleaning *Colocasia esculenta* plant leaf.
The input parameters for the equations are:

– surface chemistry, expressed by the Young contact angle (θ_o), i.e. the drop contact angle which the chemistry induces on a smooth surface;
– surface roughness, expressed by the roughness ratio r and the wetting fraction f. Both values are dependent on the sink-depth of the drop into the surface roughness.

The equations delivers:

1. energy of each drop status including metastable and global energy minima.
2. contact angle of metastable and global energy minima.
3. wetting fraction for non-wetted area of metastable and equilibrium drop shape status.

From that results, the following useful properties can be determined:
a.) wetting area of metastable and global energy minima:

$$A_{sl} = r \cdot f \cdot A_{base}^{drop} = \frac{r \cdot f \cdot (3V/\pi^2)^{2/3} \sin^2\theta}{(2 - 3\cos\theta + \cos^3\theta)^{2/3}} \tag{56}$$

where V is the drop volume.
b.) Energy barriers for wetting/dewetting and for transitions between energy minima. The energy barriers can be compared with drop fall experiments.
c.) Contact angle hysteresis, a key factor for drop roll-up (self-cleaning) ability, given by (Bhushan & Her, 2010):

$$\Delta\theta = \theta_{adv} - \theta_{rec} = f \cdot r \cdot \frac{\cos\theta_{r0} - \cos\theta_{a0}}{\sin\theta_{equil}} \tag{57}$$

where θ_{adv} and θ_{rec} are the advancing and receding angle for a rough surface, and θ_{a0} and θ_{r0} are the advancing and receding angle which the surface chemistry build-up on a smooth surface. θ_{equil} is the drop contact-angle on the rough surface, which corresponds to the status under study, e.g. metastable or equilibrium states.
d.) Adhesion tension $\tau^o = \gamma_{lv} \cdot \cos\theta$, a factor affecting biocompatibility (Parhi & Golas & Vogler, 2010; Vogler, 2001; 1998; 1992).
The generalization to hierarchical structures and various acting forces are straightforward.

8. References

Rijke A. M. & Jesser, W. A. (2010). The feather structure of dippers: Water repelency and resistance to water penetration. *The Wilson Journal of Orinithology*, Vol. 123, 563 – 568.

Mengnan Qu & Jinmei He & Junyan Zhang (2010). Superhydrophobicity, Learn from the Lotus Leaf, In *Biomimetics Learning From Nature*, Amitava Mukherjee (Ed.), ISBN: 978-953-307-025-4, INTECH, Available from: http://www.intechopen.com/articles/ show/ title/ superhydrophobicity - learn - from - the - lotus - leaf

Kenneth Denbigh (1968). In: *The principles of chemical equilibrium*, Cambridge University Press, London, New-York.

Cool Th., Bartol A., Kasenga M, Modi K, & Garcia R. E. (2010). Gibbs: Phase equilibria and symbolic computation of thermodynamic properties. *Calphad: Computer Coupling of Phase Diagrams and Thermochemistry*, Vol. 34, 393 404, doi:10.1016/j.calphad.2010.07.005

Hüger E., Kana Th., & Sob M. (2010). A mechanism of inhibition of phase transitions in nano-grained close-packed Pd thin films. *Calphad: Computer Coupling of Phase Diagrams and Thermochemistry*, Vol. 34, 421 427, doi:10.1016/j.calphad.2010.07.009

Hüger E., Rothe H., Frant M., Grohmann S., Hildebrand G., & Liefeith, K. (2009). Atomic force microscopy and thermodynamics on taro, a self-cleaning plant leaf. *Applied Physics Letters*, Vol. 95, 033701-1 – 033702-3.

Barbieri L., Wagner E. & Hoffmann, P. (2007). Water wetting transition parameters of perfluorinated substrates with periodically distributed flat-top microscale obstacles. *Langmuir*, Vol. 23, 1723 – 1734.

Patankar N. A. (2004). Transition between superhydrophobic states on rough surfaces. *Langmuir*, Vol. 20, 7097 – 7102.

Patankar N. A. (2003). On the modeling of hydrophobic contact angles on rough surfaces. *Langmuir*, Vol. 19, 1249 – 1253.

Nosonovsky M. & Bhushan, B. (2005). Roughness optimization for biomimetic superhydrophobic surfaces. *Microsyst. Technol.*, Vol. 11, 535 – 549.

Nosonovsky M. & Bhushan, B. (2006). Stochastic model for metastable wetting of roughness-induced superhydrophobic surfaces. *Microsyst. Technol.*, Vol. 12, 231 – 237.

Ishino, C. & Okumura, K. (2006). Nucleation scenarios for wetting transition on textured surfaces: The effect of contact angle hysteresis. *Europhysics Letters*, Vol. 76, 464 – 470.

Bhushan B. & Her, E. K. (2010). Fabrication of Superhydrophobic Surfaces with High and low Adhesion Inspired from Rose Petal. *Langmuir*, Vol. 26, 8207 – 8217.

Chaudhury M. K. & Whitesides, G. M. (1992). Correlation between surface free energy and surface constitution. *Science*, Vol. 255, 1230 – 1232.

Hunter L. (2010). The C-F bond as a conformational tool in organic and biological chemistry. *Bellstein Journal of Organic Chemistry*, Vol. 6, 1 – 14.

Hüger E., Zeleny M, Kana T., Osuch K. & Sob, M. (2008). A peculiar bonding of sulphur at the Nb(001) surface. *Europhysics Letters*, Vol. 83, 26001-1 – 26001-6.

Marmur A. (2010). Solid-Surface Characterization by Wetting. *Annual Reviews of Material Research*, Vol. 39, 473 – 489.

Parhi P., Golas A. & Vogler Erwin A. (2010). Role of Proteins and Water in the Initial Attachment of Mammalian Cells to Biomedical Surfaces: A Review. *Journal of Adhesion Science and Technology*, Vol. 24, 853 – 888.

Vogler Erwin A. (2001). How Water Wets Biomaterial Surfaces. In: *Water in Biomaterials Surface Science*, M. Morra (Ed.), John Wiley and Sons, Ltd, New-York.

Vogler Erwin A. (1998). Structure and reactivity of water at biomaterial surfaces. *Advances in Colloid and Interfacial Science*, Vol. 74, 69 – 117.

Vogler Erwin A. (1992). Practical Use of Concentration-Dependent Contact Angles as a Measure of Solid-Liquid Adsorption. 2. Experimental Aspects. *Langmuir*, Vol. 8, 2013 – 2020.

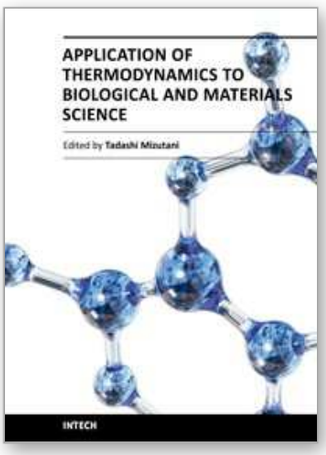

Application of Thermodynamics to Biological and Materials Science

Edited by Prof. Mizutani Tadashi

ISBN 978-953-307-980-6
Hard cover, 628 pages
Publisher InTech
Published online 14, January, 2011
Published in print edition January, 2011

Progress of thermodynamics has been stimulated by the findings of a variety of fields of science and technology. The principles of thermodynamics are so general that the application is widespread to such fields as solid state physics, chemistry, biology, astronomical science, materials science, and chemical engineering. The contents of this book should be of help to many scientists and engineers.

How to reference

In order to correctly reference this scholarly work, feel free to copy and paste the following:

Erwin Hueger, Juergen Rost, Marion Frant, Gerhard Hildebrand and Klaus Liefeith (2011). Biomimetics - Thermodynamics to Study Wetting of Self-Cleaning Surfaces, Application of Thermodynamics to Biological and Materials Science, Prof. Mizutani Tadashi (Ed.), ISBN: 978-953-307-980-6, InTech, Available from: http://www.intechopen.com/books/application-of-thermodynamics-to-biological-and-materials-science/biomimetics-thermodynamics-to-study-wetting-of-self-cleaning-surfaces

INTECH
open science | open minds

InTech Europe
University Campus STeP Ri
Slavka Krautzeka 83/A
51000 Rijeka, Croatia
Phone: +385 (51) 770 447
Fax: +385 (51) 686 166
www.intechopen.com

InTech China
Unit 405, Office Block, Hotel Equatorial Shanghai
No.65, Yan An Road (West), Shanghai, 200040, China
中国上海市延安西路65号上海国际贵都大饭店办公楼405单元
Phone: +86-21-62489820
Fax: +86-21-62489821

IntechOpen